MultiMiner Austria – Mapping Hochfilzen

Overview for geological mapping

Gerald Schuberth-Hlavač[1], Christoph Stranzl[2], Johann Raith[3], Benjamin Huet[1], Holger Paulick[1]

1. GeoSphere Austria
2. RHI Magnesita
3. Montanuniversität Leoben

2024-10-03

Version 4

Table of contents

1 Introduction

This is intended to serve as an introduction for the preparation of the geological mapping at Hochfilzen site for MultiMiner project. The areas to be mapped are defined and a brief geological overview is presented. The study area is placed in a modern regional geological framework and the rocks most relevant for the mapping work are presented.

As a base for a more in-depth familiarization, the explanations for sheet 122 Kitzbühl (Heinisch et al., 2015) and especially the rich literature list there should be mentioned. A geological overview of the magnesite deposits near Hochfilzen is given by e.g. Vavtar (1976).

Magnesite mineralizations are currently known in the Spielberg dolomite group and in the dolomite-radiolarite complex (see below). The known deposits, such as Weißenstein and Bürgl, are located in the Hochhörndler complex (Heinisch et al., 2015). Regarding the magnesite deposits in the study area, it should be mentioned that there is a discussion about their age and their genesis going back to the 19th century with significant differences of opinion. The inferred age of mineralization ranges from middle Silurian over Variscan to Alpidic and the spectrum of genesis models include primary-sedimentary, synsedimentary to early diagenetic to metasomatic. Also, there are different ideas about the origin of magnesium intake (Tollmann, 1977).
See also Section 5 on this topic.

1.1 Location of the study area

Geographically, the study area is located about five to seven kilometers southwest of Hochfilzen – see Figure 1.1. It is mostly located in the province of Tyrol and a small part is located in the province of Salzburg.

1.2 Map sheets

The areas to be mapped concern sheets 122 Kitzbühl (Heinisch et al., 2003) and 123 Zell am See (Heinisch et al., 1995). Explanatory notes (Heinisch et al., 2015) are available for the former map sheet. The boundary of the two map sheets in the study area is the, here approximately north-south oriented, Fieberbrunner Ache. The majority of the areas to be investigated are located on sheet 122.. Mentionable "sheet edge faults" between these sheets are not known in the study area and are not of major importance here because no mapping area overlaps the sheets. Important lithologies have different numbers on the map sheets, but are named roughly the same.

1.3 Questions

The basic concern of the mapping work is the magnesite mineralization. Accordingly, the focus is on geological parameters that can be assumed to be relevant as evidence for magnesite mineralization processes. Important geological features include contacts to the adjacent rocks, differences in grain sizes, faults, ...
It must be kept in mind that in the course of the MultiMiner project, the study area will be

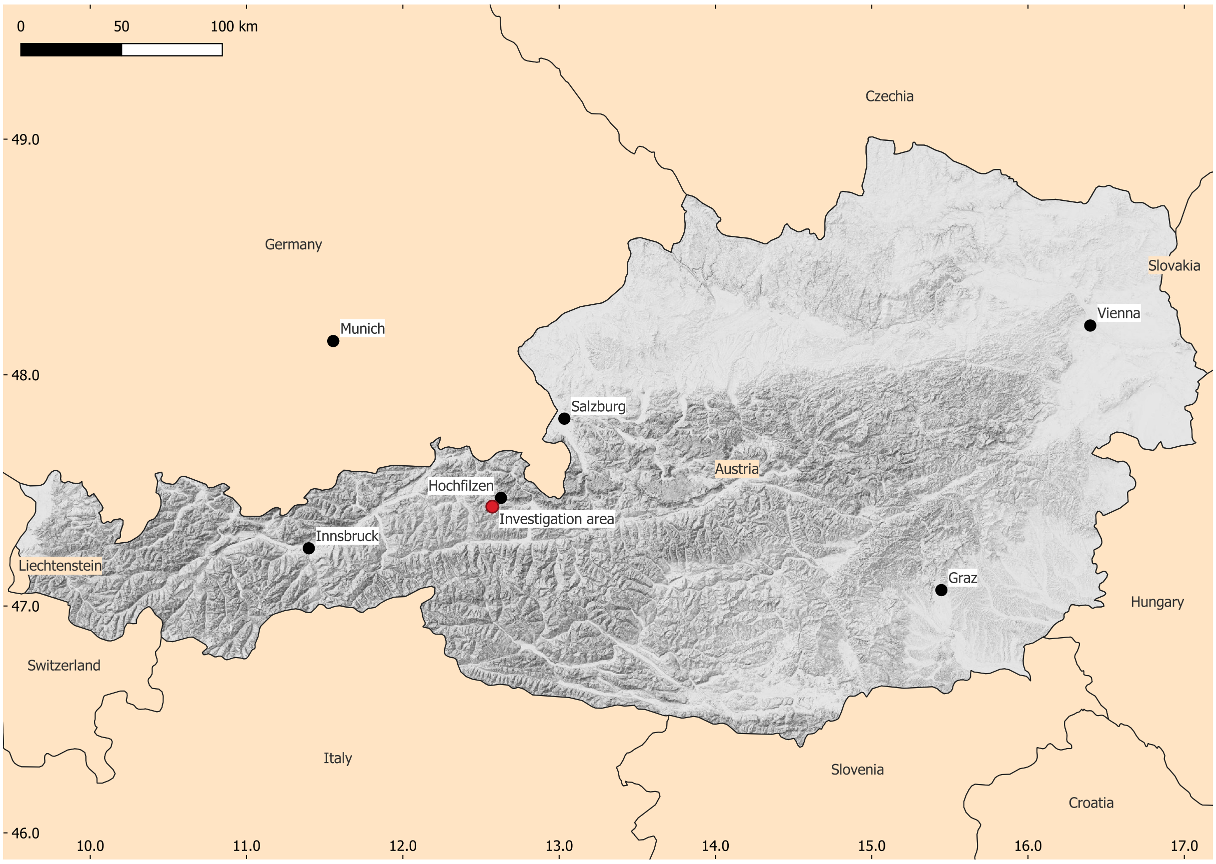

Figure 1.1: Location of the study area – marked in red (base map: basemap.at)

surveyed using spaceborne and drone-based Earth Observation (EO) methods, and the results of the mapping work will be linked to the results of these methods. In this respect, the field work should also take into account what a satellite or drone "sees" and thus, for example, not only nice outcrops should be examined, but also weathered rock.

1.4 Issues

At this point a few words about the practical field work and its preparation:

- Online, the regions and areas are shown with different map material at https://ardigeos.geologie.ac.at/mumimap.
- The mapping areas can be obtained as GeoPackage through the link https://rhea.geologie.ac.at/index.php/s/rUqqImMlXdzGAUl.
- The two map sheets can be obtained through the Tethys Research Data Repository, of Geosphere Austria, through the following links as PDFs and as GeoPackages:
  - GK 122 Kitzbühl: https://doi.tethys.at/10.24341/tethys.53
  - GK 123 Zell am See: https://doi.tethys.at/10.24341/tethys.54
- The Geological Maps of the Republic of Austria 1:50,000 can be integrated into GIS programs as raster layers via the following WMS/WMTS link: https://gisgba.geologie.ac.at/arcgis/services/image/AT_GBA_GK50/ImageServer/WMSServer?request=GetCapabilities
- WGS84, EPSG:4326, is to be used as the coordinate system for marking field points. This is the same coordinate system used by GPS devices.
- The positions of points recorded by GPS must be checked with a GIS program and satellite images (e.g. the orthophoto layer of basemap.at) and corrected if necessary prior to further use.

- Structural measurements are to be reported in (dipDirection, dip)-value pairs – as they are provided by structure compasses after Clar – and not in (strike, dip)-value pairs as it is still common in the Anglo-American area.
- The use of 10% of hydrochloric acid to distinguish magnesite from dolomite has not proved successful. This can be deceptive, as aragonite may also be present in part. Macroscopic identification of carbonates is more appropriate.
- Sample labeling should not be done on the sample with a permanent or paint marker, rather the sample should be placed in a bag and the bag should be labeled. The reason is a possible spectral analysis on the sample in the laboratory and colors added by markers could make this analysis difficult or impossible.
- For field work, the period June-July seems to be ideal, because here mostly a stable weather situation (especially July) prevails and the days are long. In August, precipitation is traditionally expected. In September, however, favorable weather conditions could arise again, although the days are already shorter at this time.

2 Regions and areas

The areas to be mapped are located in a roughly west-east oriented strip south of Fieberbrunn and Hochfilzen with the active open pit Weißenstein roughly in the middle – see Figure 2.1 and Figure 2.2. For (preliminary) structuring, the study area is divided into three regions and associated areas. These are now briefly described here – from east to west and with decreasing priority.

2.1 East Region

Lies to the east of the active Weißenstein open pit and is the only one of the regions on map sheet 123. It is bounded by the former Bürgl open pit, to the west, and Inschlagalpe underground mine, to the east. Two varieties of magnesite can be identified in this region: One fine-grained and one coarse-grained.

2.1.1 Area 1

East of the former Bürgl open pit resp. the eastern side of the Spielberggraben. This area should be easily accessible: Access via Burgeralm and parking there and on. After consultation with the landowners, it may also be possible to use the alpine path to the Kleberkopf saddle.
For parts of this area there is a detailed description and mapping by Riedler (2010).

2.1.2 Area 2

The area around the former mine site Inschlagalpe. Here, a well exposed area to the west of the former mine site is of great interest. (South)East of this, the terrain is quite steep and forested – however mapping information exists from when the mine was in operation. A relatively coarse-grained magnesite with zero porosity is found here.
Access via the Schwarzleotal with parking at the show mine Leogang. Possibly, the private road behind the gate can be used after consultation with the landowner.

2.1.3 Area 3

This is still vaguely defined. Here, laser scans should be consulted in order to identify potential outcrops. If none of them could be identified the southern border of the Spielberg dolomite should be followed.
Access via the Schwarzleotal with parking possibility at the Leogang show mine. Possibly, the private road behind the barrier can be used after consultation with the landowner.

2.2 Central Region

This region is on the eastern edge of map sheet 122. It is the area to the west and north around the Weißenstein open pit.

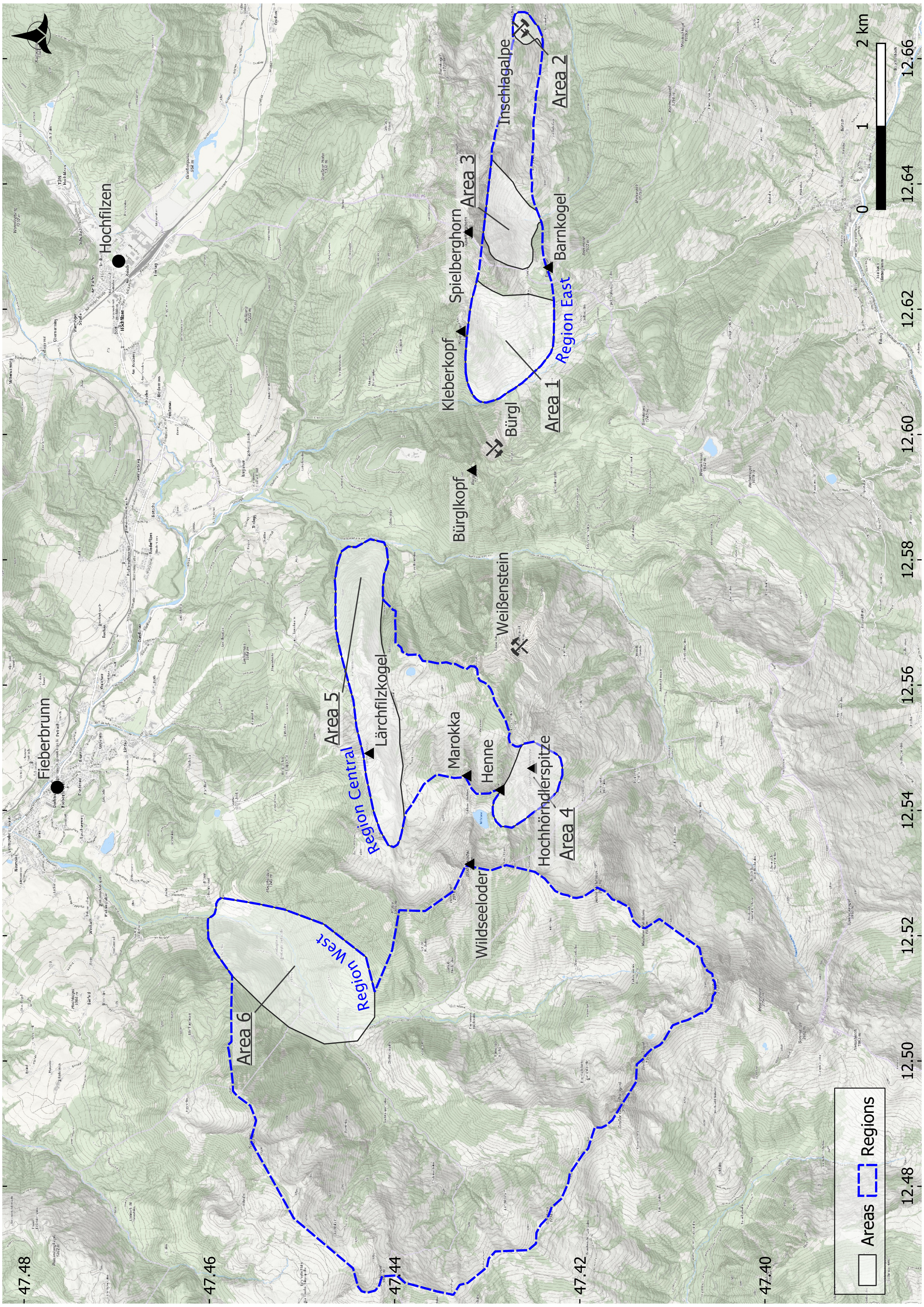

Figure 2.1: Overview of the mapping areas (base map: basemap.at)

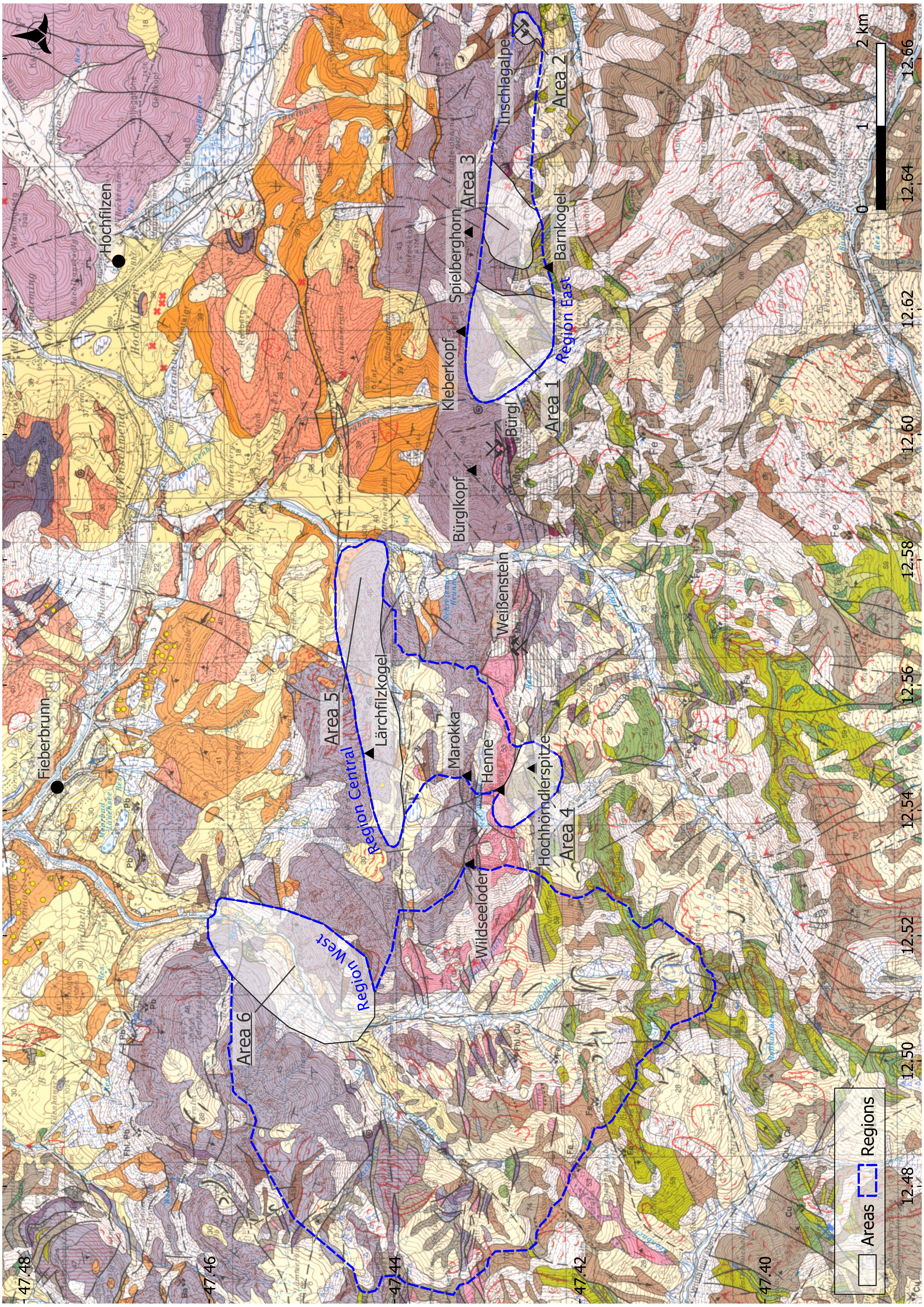

Figure 2.2: Overview of mapping areas (base map: Geological Map Austria)

2.2.1 Region 4

This is a hiking area including the Blumenweg track and some via ferrata near the ridge in the north. Of great interest here is an outcrop of black dolomite and especially its contacts with the neighbouring rock. Furthermore, this is an area where the Glemmtal complex and the Hochhörndler complex are exposed and therefore more metabasites could be found here.

2.2.2 Area 5

Along the roughly west-east oriented "ridge" at the Lärchfilzkogel down to the Hörndlingergraben. Parking is possible at the Lärchfilzhochalm and in the Hördlingergraben.

2.3 West Region

The region is located directly at the western connection to Central Region and on map sheet 122. This region is intended for model verification of spaceborne and drone-based Earth Observation (EO). The EO shall first provide indications of possible magnesite mineralization, which will subsequently be searched for.
This region is characterized by the Pletzerbach and its tributaries, the Lengfilzenbach and Grubalm with Sulztalbach.

2.3.1 Area 6

In this area Magnesite is known as rolled pieces in the bedload of the Pletzerbach creek. Their origin in the form of outcrops is not known and should be clarified if possible. In the north of the Pletzergraben mighty Spielberg dolomites are exposed. Especially their boundaries to the south are to be localized and worked on. The area is part of the Pletzergraben and should be mapped on both sides of the Pletzenbach.
This area has the lowest priority and should be mapped depending on possibilities.

3 Geological framework

On the map sheets mentioned above, the study area is located in the Wildseeloder unit ⊂ Grauwackenzone ⊂ Upper Austroalpine. Small-scale contacts with the Glemmtal unit – also graywacke zone – and the Northern Calcareous Alps ⊂ Upper Austroalpine occur.

This traditional nomenclature of geological units no longer corresponds to the current state of knowledge. According to modern tectonic nomenclature, the area under investigation is part of the Staufen-Höllengebirge nappe, which is assigned to the Tyrolian-Noric nappe system (Schmid et al., 2004; Heinisch et al., 2015; Huet et al., 2019).
An overview tectonic map of the Eastern Alps is given in Figure 3.1 and Figure 3.2 shows a schematic diagram of the major tectonic units of the Eastern Alps and the incorporation of the Tyrolian-Noric nappe system into these units (Schuster et al., 2013; Schuster and Stüwe, 2022). The palaeogeographic position of the Austroalpine from Cambrian to Devonian is outlined in Figure 3.3.
The lithostratigraphic division of Paleozoic rocks within the Staufen-Höllengebirge nappe (Huet et al., 2019, 2022) was based on the explanations of GK 122 Kitzbühl (Heinisch et al., 2015). Four complexes are distinguished, which correspond to Variscan tectonic units. From the footwall to the hanging wall, these are the following lithodemic units: Uttendorf complex, Glemmtal complex, Hochhörndler complex and Wildseeloder complex. These are unconformably overlain by Permomesozoic lithostratigraphic units.

The metamorphic history of the Staufen-Höllengebirge nappe is poorly studied. In general, it is assumed that there is an increase in the degree of metamorphism from north to south (e.g. Schlaegel-Blaut, 1990; Rantitsch and Judik, 2009; Heinisch et al., 2015). In general maximum greenschist facies pressure-temperature conditions can be assumed for the study area: Approximately in the range of 350 °C–400 °C and pressures greater than 3 kbar and less than 4,5 kbar–8 kbar (Schlaegel-Blaut, 1990 and references therein). In detail, however, it seems difficult to assign the deformations and metamorphism to the Variscan or the Eoalpin event (Huet et al., 2019).
Based on data from illite crystallinity, the degree of graphitization, the presence of chloritoid and the Conodont Alteration Index (CAI), metamorphism in the (lower) greenschist facies is assumed to have occurred during the (Cretaceous) Eoalpidian event. $^{40}Ar/^{39}Ar$ ages, from white mica fine fractions, in the 115 Ma–95 Ma range indicate cooling of the rocks of the Staufen-Höllengebirge nappe and their exhumation during this event (Schuster et al., 2004; Heinisch et al., 2015 and references therein). This metamorphism was again weakly overprinted by advective heat transport and circulating fluids during the course of the Alpine orogeny, in the Oligocene to Miocene (Rantitsch and Judik, 2009). Variscan metamorphism is not documented in the study area; however, weak (lowermost greenschist facies) prealpine deformation and metamorphism is assumed (Heinisch et al., 2015). This is consistent with $^{40}Ar/^{39}Ar$ dating (Panwitz, 2006) of detrital muscovites indicating Neoproterozoic ages (in the range 600 Ma–800 Ma). The closure temperature of muscovite in the Ar/Ar system, 390 ± 50 °C (Schaen et al., 2020), has thus not been (significantly) exceeded since that time.

Note

Regarding the terms "Greywacke Zone" and "Northern Calcareous Alps", it should be mentioned that these historical terms date from a time before today's understanding of the tectonic nappe structure of the Alps (Schuster, 2015). One can probably understand these terms as geological units in the sense that they refer to rocks characteristic for them. However, they are not tectonic or lithostratigraphic units in the strict sense (Huet et al., 2019).
The term graywacke zone describes a geographic unit (Schuster, 2015) which represents an east-west oriented strip of Paleozoic rocks. This is several hundreds of kilometers long, extends roughly from Schwaz in Tyrol to Lower Austria at the margin of the Vienna Basin, and has a maximum width of about 25 km (Heinisch et al., 2015). Based on the spatial allocation, the Western and Eastern Grauwackenzone can be distinguished.
Thus, the term graywacke zone – and the accompanying subgroups such as northern, southern, western and eastern – should be seen as an informal term without stratigraphic and tectonic implications.

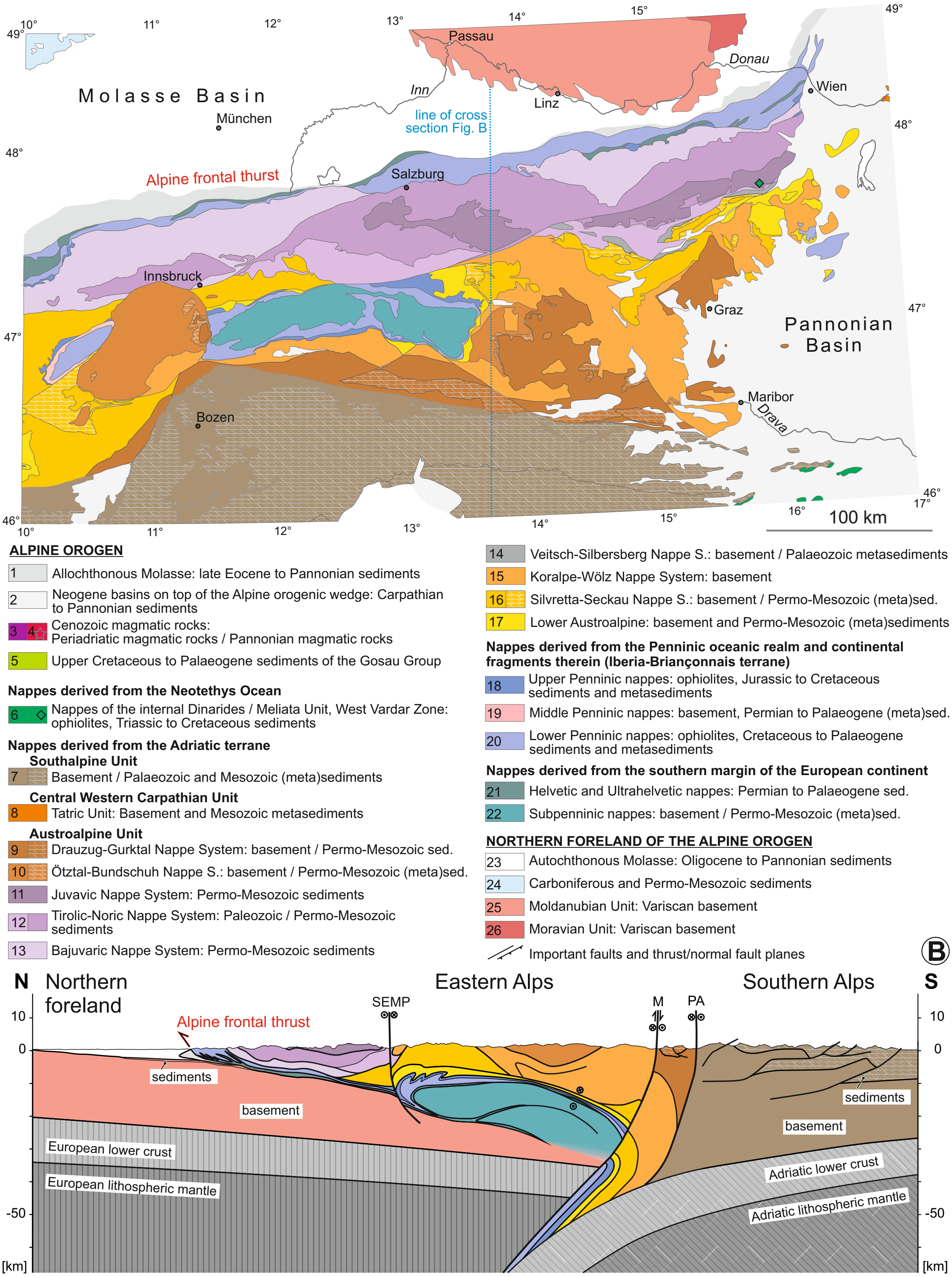

Figure 3.1: Tectonic map of the eastern Alps and the northern foreland, nomenclature after Schmid et al. (2004), Modified after Schuster et al. (2013) and Schuster and Stüwe (2022). Numbers reference to tectonic units in Figure 3.2.
SEMP: Salzach-Ennstal-Mariazell-Puchberg-, M: Mölltal-, PA: Periadriatic fault system

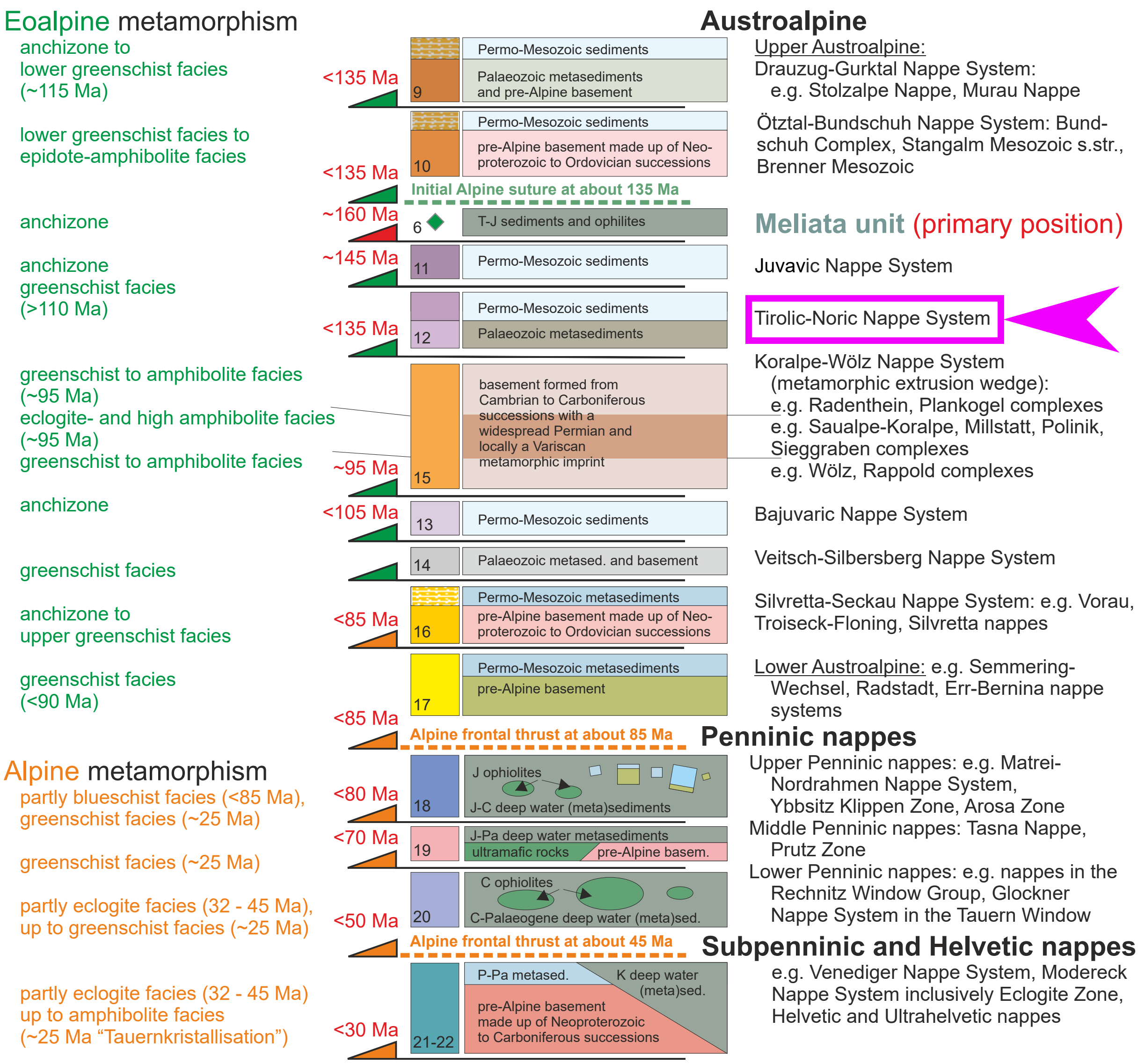

Figure 3.2: Schematic diagram of the major tectonic units of the Eastern Alps, after Schuster et al. (2013) and Schuster and Stüwe (2022). Highlighted is the Tyrolian-Noric nappe system in which the mapping area is located.
- Left: Degree of metamorphism during the Eoalpine (Cretaceous) and Alpine (Cenozoic) events and the time of peak metamorphism;
- Middle: Major lithologic content of tectonic units, red numbers indicate time of emplacement in Alpine orogen wedge, numbers in colored boxes reference tectonic units on map in Figure 3.1;. - Right: tectonic and lithostratigraphic units.
T: Triassic, J: Jurassic, C: Cretaceous, Pa: Paleogene.

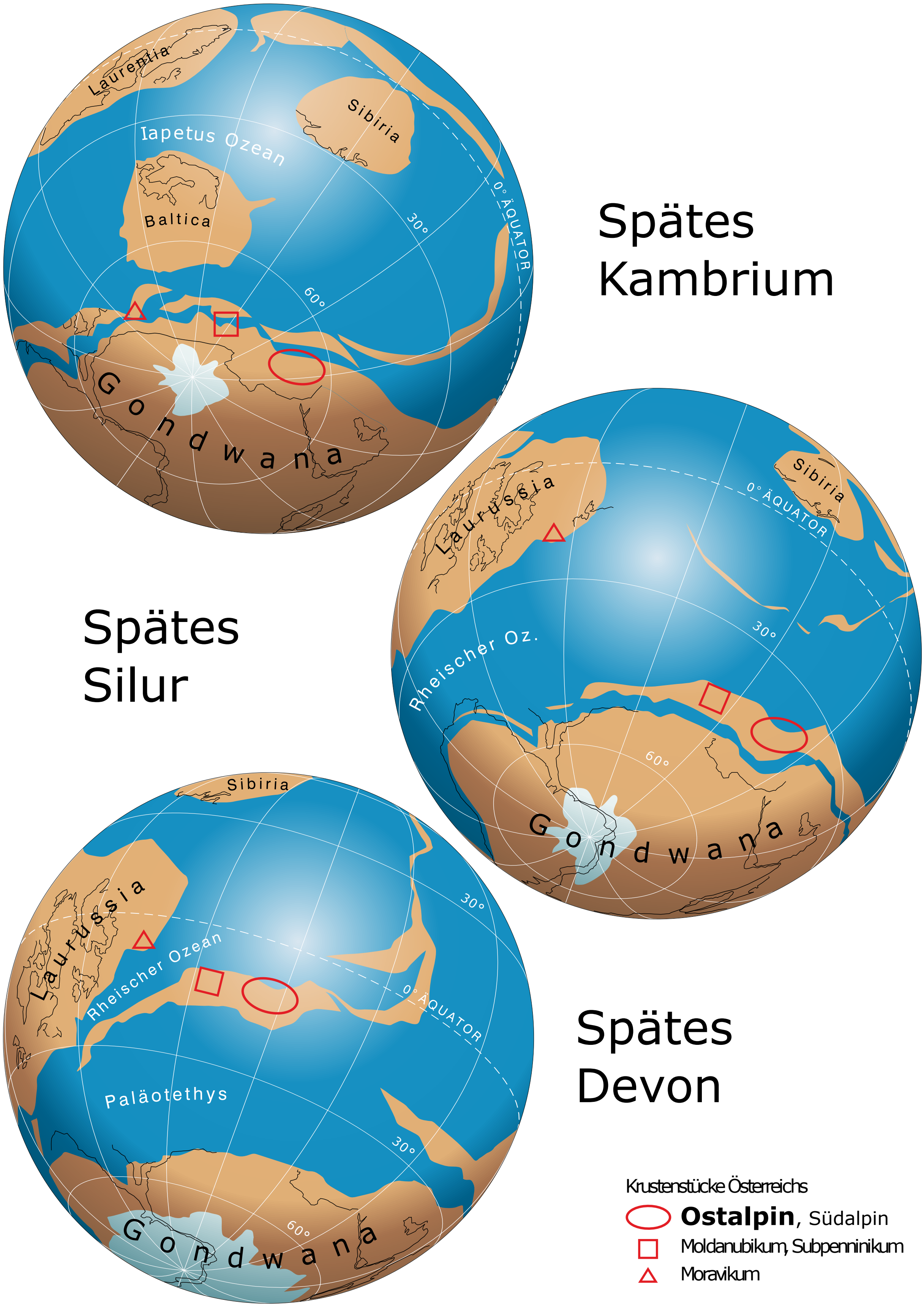

Figure 3.3: Palaeogeographic position of the Austroalpine (red ellipse) from Cambrian to Devonian. Pieces of crust split off at the northern edge of Gondwana and drift north towards Laurentia or Baltica. From an initial position near the South Pole it drifts to a position near the equator with changed climatic conditions. From Schuster et al. (2015)

4 Rock types and lithological units

Lithologically particularly relevant for the investigations here is the Wildseeloder complex, which is made up of Middle Ordovician metaignimbrite (Blasseneck porphyroid), Upper Devonian siliciclastics and various Silurian to Upper Devonian carbonate rocks – including the Spielberg dolomite group (Heinisch et al., 2015; Huet et al., 2019).
Rocks of the Glemmtal complex and the Hochhörndler complex can occur primarily on the southern edges of the areas to be examined. The Glemmtal complex comprises mostly Early Paleozoic to Lower Carboniferous mudstone, siltstone, sandstone and conglomerate with a turbiditic origin with subordinate inclusions of Ordovician and Devonian metabasites and also locally occurrences of Blasseneck porphyroid and carbonate rocks (Huet et al., 2019). The Hochhörndler complex consists of a siliciclastic matrix with isolated carbonate and magmatic elements from the Wildseeloder complex and the Glemmtal complex and it probably represents a sequence with olistoliths and/or a tectonic zone (Huet et al., 2019). Hence, rock types of the neighboring complexes are present in the Hochhörndler complex as reworked components.

In the map sheets, only the Wildseeloder and Glemmtal complexes are distinguished. These represent different facies with their specific lithologies. The Hochhörndler complex is implicitly to be understood as a "transition zone" – in which the lithologies of the other two complexes are mixed.
For practical fieldwork, the rocks can be assigned to the complexes as follows:

Wildseeloder Complex Thick carbonates and metaignimbrite, almost no basites, almost no pelites

Hochhörndler Complex Isolated, small-scale bodies of basites, carbonates, porphyroids in a matrix of siliciclastics such as slates, quartzites, ...
In the geological maps, the Hochhörndler Complex can be recognized by the fact that units of the Wildseeloder Complex lie next to units of the Glemmtal Complex without faults in between.

Glemmtal Complex Basites in carbonates and siliciclastics

Important lithologies are briefly described here and are summarized in stratigraphic divisions in Figure 4.1 and Figure 4.2.

4.1 Blasseneck porphyroid

In the study area, this porphyroid can be found, for example, at the Wildseeloder with a succession of up to 600 m thickness (Heinisch et al., 2015). It has been correlated with the Blasseneck porphyroid, named after the Styrian type locality, on the basis of lithological criteria and its stratigraphic location under the Llandovery [1] limestones (Hubmann et al., 2014).
This porphyroid is interpreted as a subaerial pumice-rich deposit, resulting from a pyroclastic density current that was washed into shallow sea basins. The volcanism is considered to be SiO_2-rich, alkaline rhyolitic to rhyolitic. Hence, the chemistry suggests an extensional regime based on the alkaline rhyolitic character. Therefore, it could have been rift-related magmatism, which led to a partial melting of the continental crust due to an increased heat flow (Heinisch,

[1] Llandovery: Lower Silurian stratigraphic series: rounded 444 Ma–433 Ma; named after the town of Llandovery in Wales

1981; Heinisch et al., 2015).
More recent investigations which include U-Pb dating from zircons and studies on zircon systematics by Blatt (2013) show ages in the range of 471 Ma–461 Ma and also suggest an interpretation of continental rifting. The paleogeographical position is assumed to be the northern edge of Gondwana.

4.2 Spielberg dolomite group

This group forms the host rock of some deposits such as siderite, baryte, fahlore and - here of particular importance - magnesite.
These dolomites represent the most important summits in the study area and form a coherent mountain range from the Kitzbühlerhorn via the Wildseeloder, the Spielbergerhorn to the Inschlagalpe. The type locality of these dolomites, the Spielbergerhorn (Hubmann et al., 2014), is one of the study area boundaries (Region 2, Figure 2.1 and Figure 2.2).
This rock group is interpreted as a Silurian-Devonian carbonate platform (Blatt, 2013) - which is now dolomitized. An age classification based on macrofossil remains, albeit sparse and weakly metamorphic, of corals, crinoids, and occasional conodonts indicates a Lower to Upper Devonian age (Heinisch et al., 2015 and references there).
The typical formation of a carbonate platform with reef complexes and a lagoon can be inferred from the rock and the fossil remains. The transition to the mainland can be seen from the inputs of clayey-sandy clastics, influences of which can be found in the upper part. The different facies manifest themselves in different forms in the dolomite rock. According to Heinisch et al. (2015), a distinction can be made between:

“Massenfazies” – massive dolomite Occasional coral relics indicate that this massive dolomite represents the reef facies of the carbonate platform

“Bankfazies” – banked dolomite The transition from the “Massenfazies” to the “Bankfazies” is differse and thus the bank thickness varies from two meters (rarely) to decimeters (more often).
This facies or this dolomite outweighs the other dolomites of this group in terms of frequency of occurrence. Due to the thickness and extent of these rocks, an extensive (Devonian) carbonate platform is assumed.
Sedimentary structures are occasionally preserved as laminites seen as remnants of algal mats from the stillwater area of a lagoon facies. Furthermore, crinoid remains can occasionally be seen, which could represent a transition from reef debris facies to reef areas.

“Flaserdolomit-Fazies” – red “Flaserdolomit” In the facies transition to the “Bankfazies”, thinnly banked colored zones occur and layers of argillaceous slate up to centimeters thick can be observed. The red color of the “Flaserdolomit” can be seen as an aeolian input of desert dust.

“Dolomit-Sandstein-Folge” Banked dolomites alternate with quartz sandstone banks and clay slates. Quartz clasts have also been found within the dolomites. Together with the “Flaserdolomit”, this sequence is interpreted as a terrigenous sedimentary input from an adjacent continent. In terms of facies, these two dolomites could represent the transition from the lagoon facies to the beach area.

Overall, the Spielberg dolomite group represents a shallow water facies close to the coast on the northern edge of Gondwana (e.g. Blatt, 2013; Heinisch et al., 2015 and references there). For sketches and more information about such a possible deposition space, see e.g. Nichols (2009), Boggs (2009), McCann and Manchego (2015) or Wikipedia.

4.2.1 Südfazies

A term that appears in the (older) literature is the so-called "Südfazies", which goes back to Mavridis (1969). He divides the carbonate rocks, in the area between Wörgl in the west and Bischofshofen in the east (Haditsch and Mostler, 1970), into two facies for the first time: the "northern facies" and the "southern facies". These two facies were describes as both lithologically and stratigraphically distinct and separated by a somewhat west-east oriented fault. Mostler (1970) also saw a "dolomite barrier" between the northern Spielberg dolomite and the Südfazies. The term Spielberg dolomite was introduced for the northern facies and its stratigraphic range was defined as Emsian to Eifelian (upper Lower Devonian to lower Middle Devonian). The southern facies has been defined as an association of distinct dolomites (stratigraphically ranging from footwall to hanging wall): black dolomite, light gray dolomite and red "Flaserdolomit", and light to dark gray coarse sparry dolomite. The stratigraphic range of these dolomites extends from the Younger Silurian (Ludlow) to the Upper Devonian (Mavridis, 1969).
In the classification of the current map sheets (Heinisch et al., 1995, 2003) and the explanations (Heinisch et al., 2015) the term "Südfazies" is no longer in use. Rather, parts of the "southern facies" were included in the Spielberg dolomite group and the black dolomite mentioned was assigned to the Dolomit-Kieselschiefer complex. The term "Südfazies" is also not found in the current (revised) stratigraphic table (Hubmann et al., 2014), but is mentioned there as a synonym for some lithologies.
Consequently, the term "Südfazies" should also be avoided when working on the MultiMiner project. However, what can be relevant for the work here is the distinction of the different dolomites as reef and basin sediments (SiO_2-bearing dolomites, siliceous slate layers, ...).

4.3 Slate

In association with the Spielberg dolomite, alternating layers of slate occur occasionally. In the hanging wall of the platform dolomite, a smooth transition into these very fine clastic sediments can be observed. Due to the macroflora residues contained in this slate, its age can be narrowed down to the Upper Devonian or younger (Heinisch et al., 2015).

4.4 Radiolarite

Associated with the banked and massive dolomite sequences of the Spielberg dolomite group, alternating sequences of black, banked dolomite, radiolarite (lydite), black slate and gray clay slate can occasionally occur. These occurrences can be assigned stratigraphically at the base of the carbonate platform, but also represent décollements and are found along faults or as small rock bodies (Heinisch et al., 2015). Chronostratigraphically, this alternation sequence is assumed to belong to the middle to younger Silurian – middle Wenlock to lower Ludlow – and its origin is considered to be a deep marine environment with euxinic conditions (Hubmann et al., 2014).
The black dolomite mentioned above should be particularly emphasized here, as it is the (main) carrier rock of the magnesite mineralization at the Weißenstein.

4.5 Metabasites of the Glemmtal complex

The metabasites are marked in the maps as metabasalt, metatuff, metatuffite, and gabbroic and dioritic dykes. This suggests some diversity in terms of volcanic genesis. Compared to recent volcanic provinces, analogies to pillow and sheet lava stacks, different variants of basaltic pyroclastics, epiclastic rearrangements and subaquatic eruptions with different production rates

can be identified. These volcanics are variously intruded by gabbroic rocks. Here, sills and vertical dykes as well as stock-like intrusions occur (Heinisch et al., 2015).
To sum it up, these metabasites can be interpreted as a product of multiphase basic volcanism with subvolcanic intrusives. Detailed geochemical investigations by Schlaegel-Blaut (1990) were able to rule out connections between volcanism and active plate boundaries – both oceanic ridges and subduction zones. Rather, they suggest a basic intraplate volcanism, which represents volcanic high zones (seamounts, island volcanoes) in a shallow marginal sea.
In summary, these metabasites are interpreted by Heinisch et al. (2015) as mostly shallow marine seamounts. Biostratigraphically, this event can be assigned to the Lower Devonian based on conodonts. Furthermore, the Glemmtal complex is described as basin facies.
Geochronological dating of these rocks using the U/Pb and Sm/Nd methods yielded ages in the range of 492 Ma–454 Ma (Heinisch et al., 2015 and references there). This covers a broad period from the late Cambrian to the middle Upper Ordovician and is in contradiction to the conodont stratigraphic classification given above. According to Heinisch et al. (2015), this contradiction must be considered open.

Note on geological vocabulary

Regarding the subvolcanic intrusives mentioned above, it should be noted that in the literature they are partly summarized as basaltic-gabbroid material and also as diabase (schist). The former is supposed to express the transitional character of the fabric of subvolcanics. Subvolcanites are intrusive rocks formed by cooling and crystallization below the surface of the earth – but at shallower depths and usually with smaller volumes than typical plutonites. Their fine-grainedness is often not as pronounced as that of the volcanic rocks and they represent transition from the volcanic rocks to the plutonic rocks. These relatively coarse-grained basaltic rocks, often with an intergranular to ophitic texture (Vinx, 2015), are called dolerites or micrograbbros (grain size over three millimeters). The term diabase, which is often used synonymously, should be avoided due to its ambiguity (Le Maitre et al., 2002).

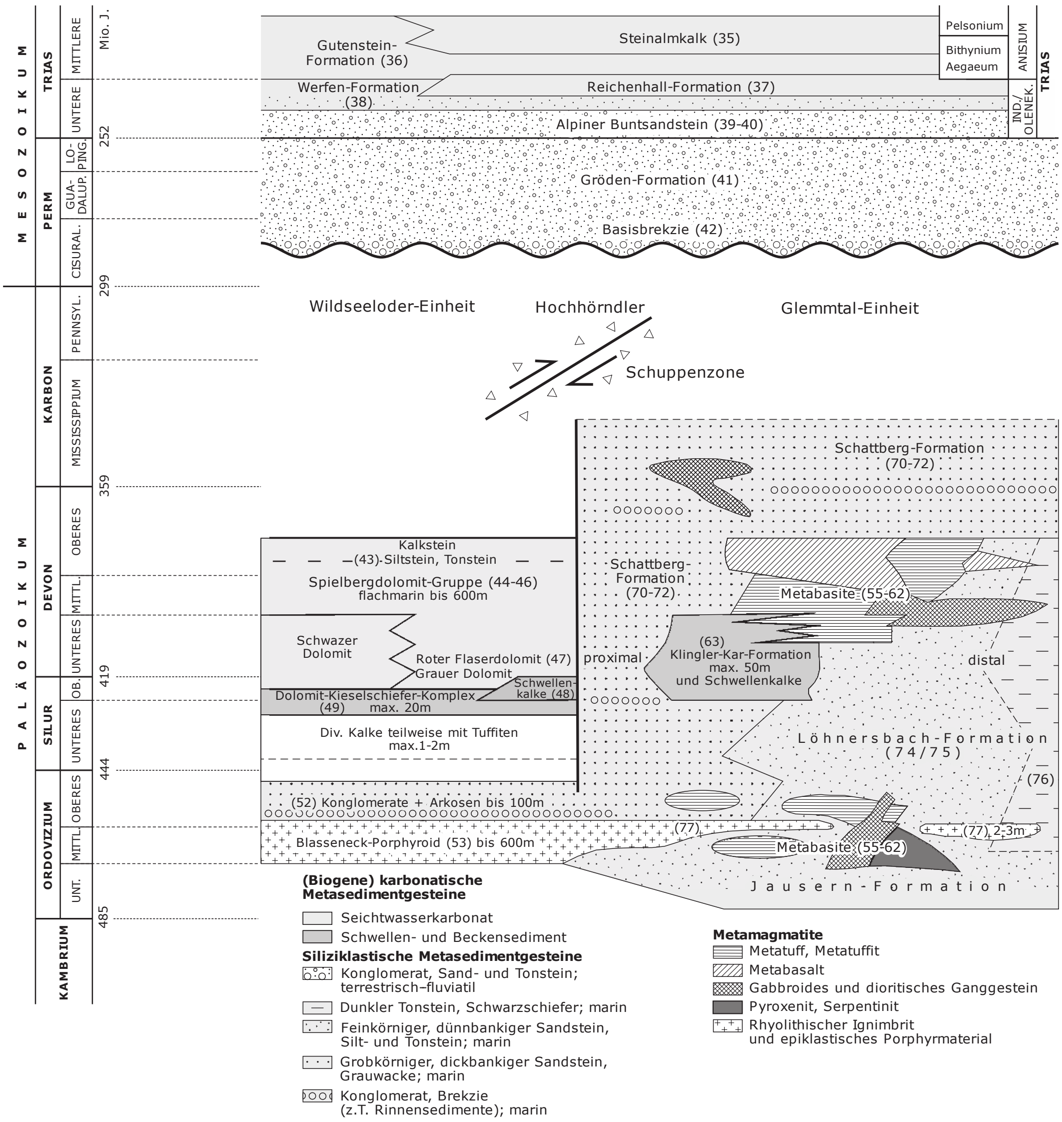

Figure 4.1: Lithostratigraphic table of the Staufen-Höllengebirge nappe, from (Heinisch et al., 2015). Left: Wildseeloder complex with dolomites of the Spielberg dolomite group and the Dolomit-Kieselschiefer complex; Right: Glemmtal complex with basites; Center: Hochhörndler complex; Blasseneck Porphyroid is found in all units. Variscan tectonics and a Permomesozoic covering are also shown

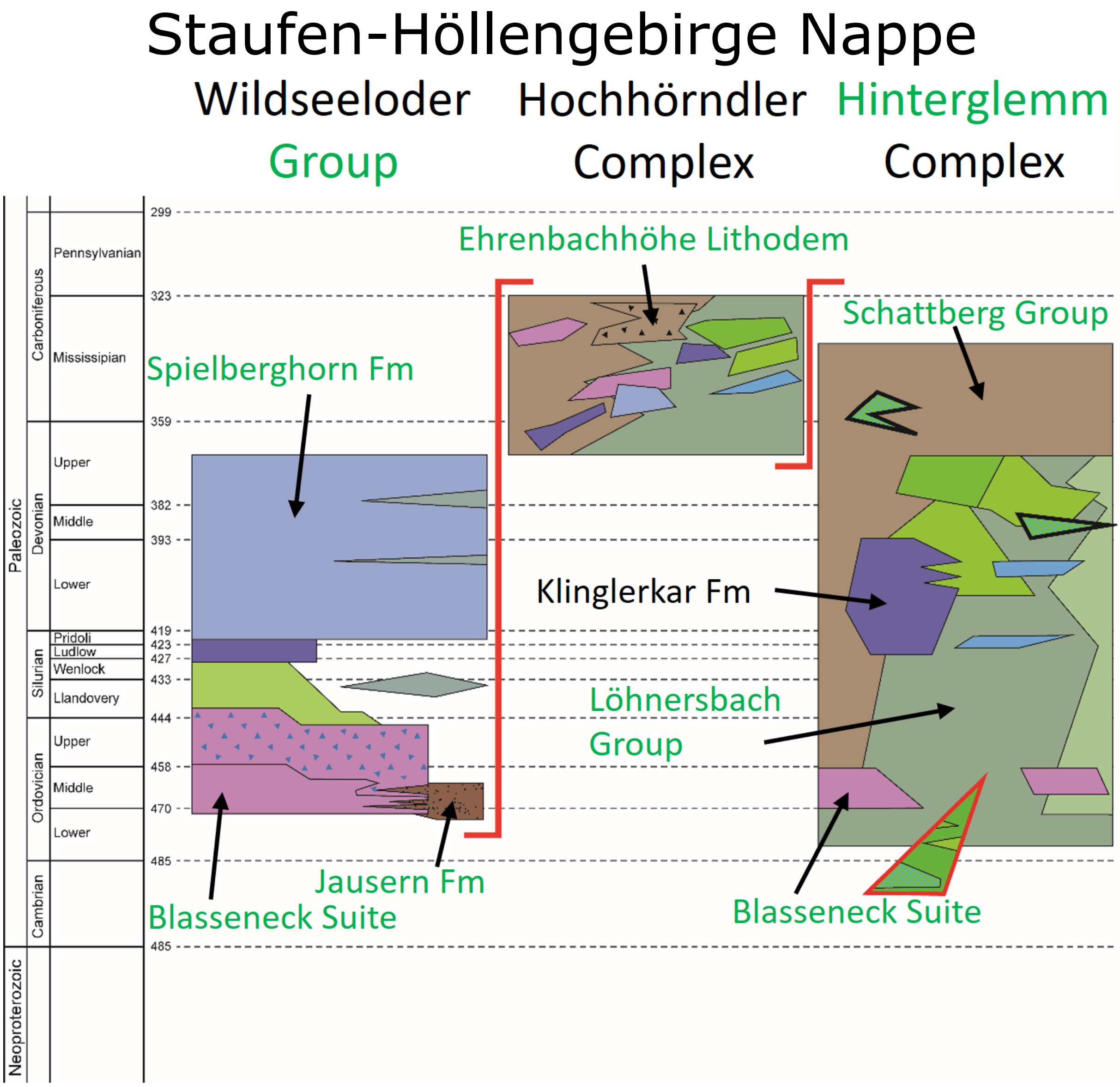

Figure 4.2: Modern lithostratigraphic model of the Staufen-Höllengebirge nappe, modified after (Huet et al., 2019, 2022); Green: proposed new denotations, for the units according to Heinisch et al. (2015) (see Figure 4.1), following a modern lithostratigraphic resp. lithodemic nomenclature (North American Commission on Stratigraphic Nomenclature, 2005). Detailed lithostratigraphy of each complex in Figure 4.3, Figure 4.4, Figure 4.5

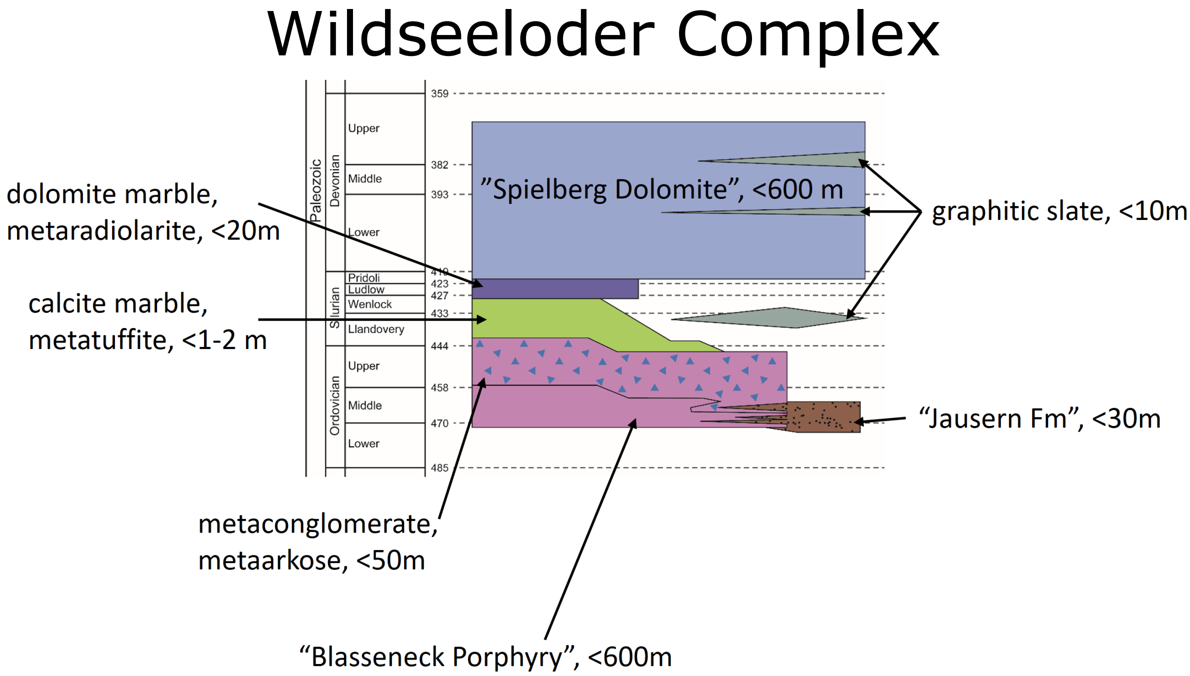

Figure 4.3: Lithostratigraphy of the Wildseeloder complex, modified after (Huet et al., 2019, 2022)

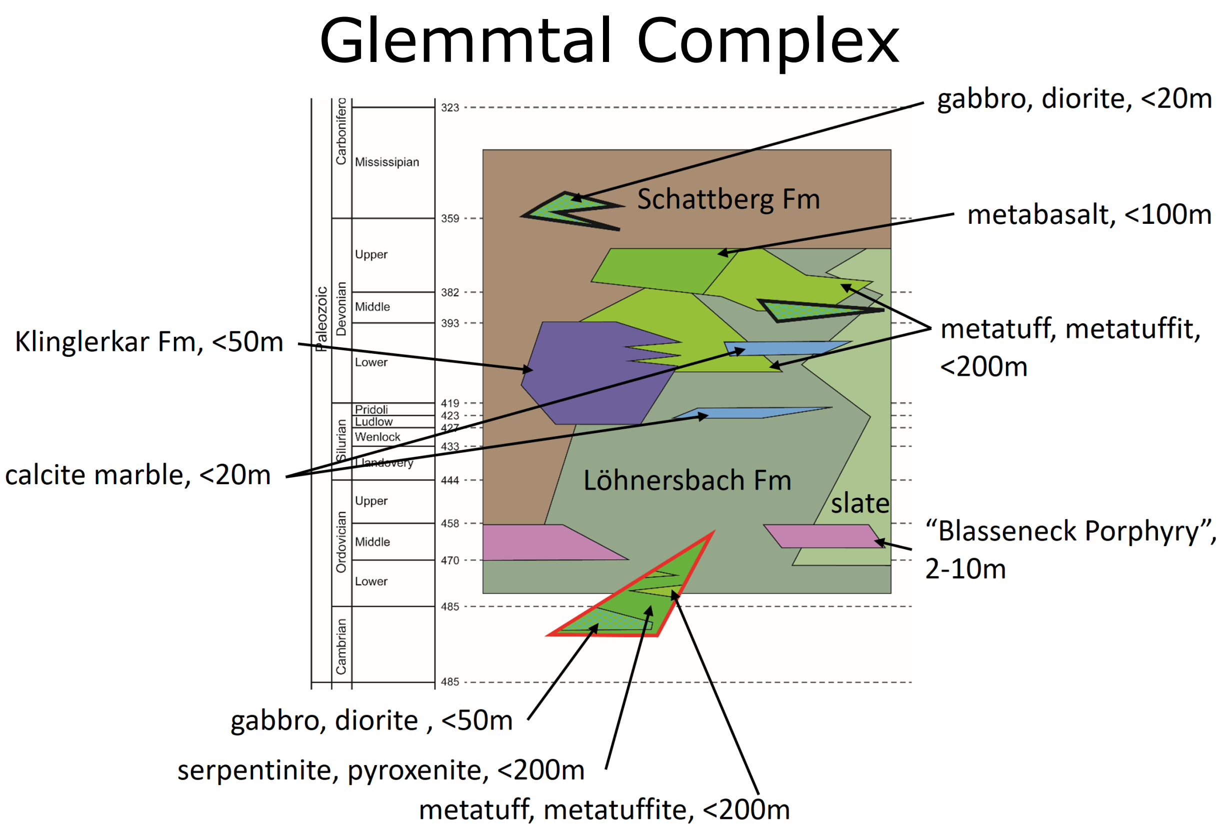

Figure 4.4: Lithostratigraphy Glemmtal complex, modified after (Huet et al., 2019, 2022)

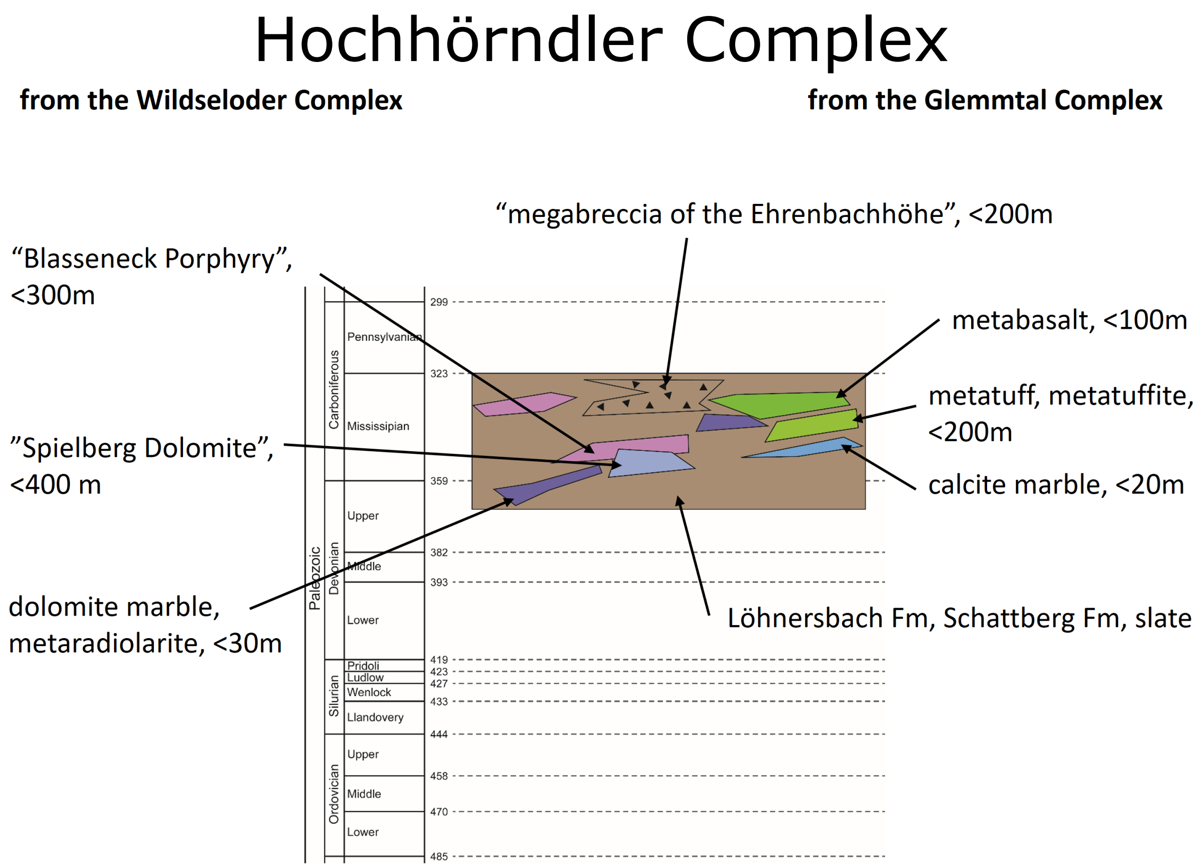

Figure 4.5: Lithostratigraphy of the Hochhörndler complex, modified after (Huet et al., 2019, 2022)

5 Magnesite deposits in the Hochfilzen area, Eastern Alps: Genetic considerations

Worldwide, most economic magnesite deposits are either of the cryptocrystalline Kraubath type or the sparry Veitsch type. Magnesite formed in sedimentary lacustrine environments only plays a subordinate role (Pohl, 2020).

Cryptocrystalline magnesite of the Kraubath type (named after an occurrence in Styria, Austria) occurs as white and very fine-grained masses (bone magnesite) in veins, stockworks and massive bodies within (meta)ultramafic rocks. It is the product of low- to moderate-temperature reactions between Mg-rich rocks and CO_2-rich aqueous fluids of hypogene or supergene origin (e.g. Pohl, 1990). Sparry magnesite of the Veitsch type (named after an abandoned mine in Styria, Austria) forms irregular to strata-bound bodies that are preferentially hosted in carbonate-dominated sequences. Deposits of this magnesite type are massive, commonly coarse-grained and often show a sparry to pinolitic texture. Marine clastic to carbonate shelf sediments are the most common precursor rocks which are transformed by Mg-rich fluids in a process known as Mg-metasomatism. Metasomatic replacement textures are widely documented in these deposits, but the timing, the nature of the fluids, the source of magnesium and the exact pressure, temperature and chemical (pTX) conditions of magnesite formation are a matter of debate since more than 150 years. Historically, two schools evolved that either propagated epigenetic (metasomatic-hydrothermal) or syngenetic (sedimentary to early diagenetic) models – for a review see Deelman (2020).

Most magnesite deposits in the Eastern Alps are of the sparry Veitsch type and occur in carbonate-dominated Paleozoic formations within the tectonic highest Austroalpine geological, i.e., the Veitsch-Silbersberg nappe system, Tirolian-Noric nappe system (geographically "Greywacke Zone"), or the Graz Paleozoic nappe complex. The magnesite deposits and their country rocks commonly record low-grade to rarely medium grade pre-Alpine and Alpine regional metamorphism.

The main deposits currently mined by RHI Magnesita in Austria are located at Breitenau (Styria), in the Hochfilzen area (Tyrol) and at Radenthein (Carinthia). Smaller active mining operations of other companies are located at Oberdorf an der Laming and Hohentauern in Styria. The total annual Austrian magnesite production in 2022 was about 844 000 t (Mayer-Jauck and Schatz, 2023).

Magnesite deposits in the Hochfilzen area are situated in the Tirolian-Noric nappe system (geographically "Northern greywacke zone") and include several active and abandoned mines at Weißenstein, Bürgl, and Inschlagalpe. These mines stretch along a ca. 6 km long corridor that is associated to the tectonically complex Hochhörndler complex (see Section 4). The carbonate host rocks are mainly dolostones and limestones of Silurian to Early Devonian age. Previous studies distinguished a northern reef-dominated dolomitic facies (Early to Middle Devonian Spielberg Dolomite) and a southern facies ("Südfazies") of Silurian fossiliferous limestones to Early Devonian dolostones (Mavridis and Mostler, 1971) – see also Section 4.2.1. According to Mostler (1970), the magnesite deposits are restricted to the southern facies.
It is to be noted that the magnesite deposits in the western "Greywacke Zone" formed in different lithologies and in carbonate sequences of different stratigraphic age (Mostler, 1973). Hence, they are not strictly stratiform but strata-bound, at best. The magnesite deposits have been affected by low-grade greenschist facies metamorphism as indicated by chloritoid, pyrophyllite

and paragonite in the surrounding metapelites (Morteani, 1989; Morteani and Neugebauer, 1990).

The spatial vicinity of the magnesite deposits in the western "Greywacke Zone" to tectonic nappe boundaries was pointed out in previous studies (Mostler, 1973; Morteani, 1989). Variscan thrust planes were thought to be possible fluid pathways for the Mg-rich mineralizing fluids in a metamorphic-metasomatic model. In this metamorphic-metasomatic model the replacement of dolomite by magnesite is controlled by inversion of the temperature gradient due to tectonic overthrusting and influx of Mg^{2+}-rich fluids from the overthrust unit (Morteani, 1989; Morteani and Neugebauer, 1990). The rare earth element (REE) contents and patterns of magnesite compared to those of the meta-sedimentary carbonate host rocks support this interpretation (Morteani et al., 1982).

Magnesite from the Weißenstein quarry is macrocrystalline but it lacks the cm-sized sparry magnesite texture that is typical for many other deposits. Banding is rarely preserved in finer grained magnesite. It has been interpreted as relict of an older sedimentary fabric whereby indicating an initial stage of sedimentary magnesite formation prior to subsequent metamorphic recrystallization (Vavtar, 1976; Schulz and Vavtar, 1989).

Magnesite was also reported from the Permian Gröden Formation (redbed sediments), which unconformably overlie the Early Paleozoic strata hosting the sparry magnesite deposits in Hochfilzen area. These Permian magnesites occur as nodules, in discrete layers within mudstones as well as intergranular cement (Spötl and Burns, 1994). Magnesite in these redbed sediments formed diagenetically in a playa-lake system and the magnesium was derived from weathering of Devonian dolostones and associated magnesite deposits (Spötl and Burns, 1994). Magnesite was also documented in the Permian basal breccia – Brunnsink breccia – (Siegl, 1953; Angel and Trojer, 1955). This breccia contains magnesite-bearing clasts, which were interpreted as sedimentary components and provided a key argument for supporting the pre-Permian (Variscan) age of the magnesite formation in the Alps (Angel and Trojer, 1955). However, detailed textural observations indicate that magnesite formation in this breccia is in fact post-depositional (Siegl, 1964; Mostler, 1970).
It remains an interesting question if and how the processes forming the sparry magnesite deposits in the Hochfilzen area and those in the Permian formations are genetically linked.

Some progress in our understanding of the fluids involved in the formation of sparry magnesite deposits comes from crush-leach analyses (Prochaska, 2001). Na/Br vs. Cl/Br plots generated by this method reveal that sparry magnesites plot at the end of the seawater evaporation trend indicating that the saline fluids ("bittern brines") derived from strongly evaporated seawater (Prochaska, 2016). The few conventional fluid inclusion studies done on magnesite deposits in the Eastern Alps confirm that the mineralizing fluids are saline aqueous brines belonging to the H_2O-NaCl system (Azim Zadeh et al., 2011). The temperatures obtained from microthermometry seem to reflect the metamorphic grade of the deposits (i.e., the fluid inclusions have undergone at least partial metamorphic re-equilibration).

Establishing a correct genetic model for sparry magnesite deposits in the Eastern Alps strongly depends on availability of reliable age data. So far only a very limited number of age data is available. The most precise age was determined in the Breitenau deposit where magnesite formation was dated at 229,3 ± 2,4 Ma with the Sm-Nd method (Henjes-Kunst et al., 2014). This Middle to Upper Triassic age invalidates models of orogenic (Variscan, Alpine) magnesite formation as repeatedly proposed in the historic metasomatic models. Instead, the formation of sparry magnesite deposits must be seen in the larger geodynamic context of lithospheric extension with enhanced crustal heat flow due to the break-up of Pangea and formation of the Neotethys.

It must be stressed that neither modern fluid inclusion studies nor age data are yet available for the Hochfilzen deposits. Both would be required to establish a sound genetic model that could be the basis of future exploration and help in interpretation of airborne data.

6 Rock descriptions

To give an impression of the main rock types in the study area, the descriptions given by Heinisch et al. (2015) where extracted and translated. Further detailed rock descriptions are given, for example, by Vavtar (1976) and Schlaegel-Blaut (1990).

6.1 Blasseneck porphyroid

Lithology numbers (53 | 49) in sheet (122 | 123)

> “In the field, the light-colored, rather coarse-banked to massive protrude rocks can be mapped well. A pastel green to yellowish color is characteristic. The porphyry structure is perfectly preserved or also heavily overprinted depending on the degree of alteration and deformation. The macroscopically recognizable, mm-sized porphyroclasts are recognized in the thin section as quartz and alkali feldspar. Idiomorphic forms (high quartz), some with magmatic corrosion bays, are common. Alkaline feldspar generally shows perthite texture, with individual domains being sericitized to varying degrees. Plagioclase occurs only subordinately and is always strongly altered. The matrix is composed of a fine felt of quartz, albite, sericite and possibly chlorite. Idiomorphic zircons demonstrate the primarily magmatic character. [. . .]
>
> The variable content of xenolith fragments compared to phenocrystals can be used for a first field differentiation (of the lithotypes). Almost crystal-free, dense porphyroid layers, yellow-green in appearance, can also be distinguished. These, as well as thinner layers, are usually heavily foliated and have conspicuously shiny silvery discontinuities, some of which appear as soapy seperation surfaces.
>
> In the ideal case, however, the rocks crumble in a coarse-blocky and gneiss-like manner and then form detrital material for local moraines (Wildseeloder). They can be traced to the foothills of the alps as the main drift. [. . .]
>
> Especially on the Wildseeloder, volcanological details can still be recognized in the field today.”

6.2 Spielberg dolomite group

Lithology numbers (44-47 | 42-44) in sheet (122 | 123)

> “These are dolomite rocks of different characteristics in their facies with a thickness of up to 600 m. This creates a typical weathered dolomite landscape, which is initially rounded off by glaciers, tends to form debris and only supports sparse vegetation. The karstification that occurs throughout leads to corresponding dry vegetation. [. . .]
>
> The rocks are greyish when weathered, but mostly rust-brown in colour, and are occasionally covered with map lichen. Freshly broken, they appear pure white to pale pink, occasionally also light grey. Primary sedimentary structures are extremely rare due to diagenetic recrystallization and metamorphic overprinting.

Mineralogically, it consits predominantly of dolomite with admixtures of ankerite or iron-rich dolomites. This causes the weathering color, which is often rusty brown. Calcite rarely occurs. The grain size ranges from 0,1 mm to 1 mm. The rocks can therefore be described as dolomite marble. Gritted decay and sanding are common secondary effects within this grain size."

Dolomit-Sandstein-Folge #44: "Well bedded dolomite alternates in layers with quartz sandstone beds and slates. Microscopic quartz clasts can also be found within the dolomite beds."

Banked Dolomite (#45): Shows "[...] bank thicknesses from 2 m to decimeter bank thickness. The latter case is the more common. [...] In favorable cases there are relict sedimentary structures preserved in the form of laminites [...]. In other cases, fragments of crinoid calyxes and crinoid stalk segments are found [...]".

Massive Dolomite (#46): This dolomite "[...] segregates in coarse blocky. Karst vents are common, as is striation. Irregular fracturing is common. Occasional relics of coral [...]" may occur.

Red Flaserdolomit, Flasermarmor with violet slate (#47): These "[...] stand out because of their intense play of colors (white-violet), their cm-thick banks and their mostly wavy, flaky structure. [...] The content of clayey material varies greatly, there can even be cm-thick slate interlayers. [...] Occasionally, the violet slates are also secondarily bleached, giving the rock assemblage a green-grey colour."

Note: According to Heinisch et al. (1995), the massive dolomite can be a carrier of magnesite mineralization – e.g. deposits Bürgelkopf and Inschlagalpe – and is therefore of particular importance.

6.3 Slate combined with Spielberg dolomite

Lithology numbers (43 | 41) in sheet (122 | 123)

"Gray argillaceous slate occasionally occurs in alternating layers with Spielberg dolomite (43) (to the west of"Platte" (mountain) in the direction of Pletzergraben, Malernalm near Kitzbühel). However, they also develop in the hangingwall with a sedimentary transition from the platform dolomites. A corresponding profile can be found on the Wildseeloder, to the south of the Griessenbodenalm. Here it can be shown that these are the youngest preserved sedimentary sequences of the Wildseeloder unit below the Variscan angular unconformity."

6.4 Dolomite-radiolarite complex

Lithology numbers (49 | 46) in sheet (122 | 123)

"Alternating sequences of dolomites, radiolarite (lydite), black shale and gray slate, which are summarized as the Dolomit-Kieselschiefer complex (49). [...] They often function [...] as décollement and can be found along faults (e.g. Lämmerbichlalm) or in rock slices (e.g. Lachtalbach, Römerweg-Barmleiten, Brunnalm, Jufenkamm). The common characteristic of the alternation is the black colour, due to the high proportion of organic carbon. Banked up to decimeters, dark, sugar-grained dolomite alternates in layers in the cm to dm range with lydites and black shales. Gray slates are also intercalated. In view of the perculiar colouration, the usually thin sequence forms a well mappable guiding horizon. Maximum thicknesses of up to 80 m are known. However, given the tendency for internal small folding, thrust tectonics and décollement, stratigraphically undisturbed profiles are very rare. This is due to the high contrast in consistency to the often neighboring banked and massive dolomite sequences."

6.5 Metabasalts of the Glemmtal complex

Lithology numbers (55, 57, 58, 59 | 50, 51, 52, 55) in sheet (122 | 123)

6.5.1 Metabasalt, massive or with a pillow structure

Lithology numbers (55 | 50) in sheet (122 | 123)

> "Metabasalts (55) can be found in the entire Glemmtal unit, with primary structures and fabrics (pillows, bubbles, glass edges) commonly preserved. Connected metamorphic lava sequences reach a maximum thickness of 300 m. [. . .]
>
> The pillows show sizes of maximum 1.5 x 1 m and minimum 0.3 x 0.1 m. A clear variation of the pillow size from the footwall to the hanging wall was not detectable in any of the sequences, however, multiple shifts between layered and pillow lavas can be observed. Due to the concave top, convex bottom and adaptation to the predefined morphology at the base of well-preserved pillows stratigraphically direction in some places can be shown. This agrees with the results from the biostratigraphically datable profiles. In other cases, the tectonic reshaping of the pillow structures made interpretation difficult. Occasionally relict glass fragments are preserved in the metabasalts. These appear dense, dark gray to black and are 1–3 cm across. The former glass is fully devitrified and transformed into a fine fringe of chlorite and ore pigment.
>
> Two types of metabasalt can be distinguished macroscopically. Both occur as metamorphic pillow lavas and layered lavas. Dark gray to dark green, irregularly breaking rocks are partly developed as "Diabasmandelstein" ("amygdaloidal diabase"); they have numerous filled bladder shaped cavities averaging around 0.3 cm in diameter. Light grey, very hard, splintery and sharp-edged types, on the other hand, occur in the lower Saalachtal (sheet 123 Zell am See). The latter show a lower proportion of bubbles.[. . .]
> The thin section investigations show pyroxene and plagioclase as well as pseudomorphoses after clinopyroxene, orthopyroxene, olivine and plagioclase as phenocrystals. Plagioclase, hornblende, chlorite, epidote, sericite, calcite, leucoxene, stilpnomelane, clinozoisite and quartz can be observed in the matrix. The content of phenocrysts and their grain size vary greatly, with phenocryst-rich and aphanitic textures present. The phenocrysts are a maximum of 7 mm long. They are often completely replaced by secondary minerals."

6.5.2 Metatuff (pyroclastic volcanic rock)

Lithology numbers (59 | 55) in sheet (122 | 123)

> "Vulcaniclastic rocks can occur both in association with the metabasalts and in layers in the metasediments. These are volcanic slate, which often still contain identifiable components. For example, the primarily pyroclastic nature of the components can

be demonstrated, e.g. as lapilli or scoria. In other cases the volcanic fragments are clearly epiclastic.

[. . .]

The lion's share of pyroclastics is found in the fine fraction (coarse ash to fine ash tuff). These occur today as dull green to blue-green appearing volcanic slates. They make up the main part of the outcrop area, for example at the end of the Glemmtal valley or along the Pass-Thurn-Straße south of Jochberg. As a rule, they show clear foliation; parts that occasionally appear more massive represent former coarse ash tuffs and are easily confused with layered lava flows. Microscopically, the mineral composition is poorly resolvable. It is a fine felt of chlorite, epidote, albite and occasionally calcite. Fine pigmentation by opaque minerals is the rule. Phenocrystal relics are almost always metamorphically altered."

6.5.3 Gabbroid dykes

Lithology numbers (57 | 51) in sheet (122 | 123)

"Metamorphic gabbroid rocks (57) occur unconformably as dykes or stock-like masses and concordantly as sills throughout the Glemmtal unit (thicknesses often in the meter range, rarely more than 10 m up to a maximum thickness of about 100 m). In the front part of Glemmtal a close association of gabbroid sills and metamorphic basaltic lavas is characteristic [. . .]. In the remaining areas, metamorphic basalts and metagabbros are found less frequently together. Concordant and discordant dykes or stocky gabbroic intrusive rocks were mapped within the metamorphic volcaniclastic rocks or within the siliciclastic metasediments[. . .] Some dykes are only dm thick, in which case they can easily be mistaken for greywacke beds.

[. . .] The macroscopic and microscopic appearance of the metamorphic gabbroid intrusives is very different. In outcrop, these rocks appear massive, dark green to grey. Grain size and structure vary from uniform (coarse, medium to fine-grained) to porphyry-grained with maximum 1.5 cm long pyroxene crystals. A wide range of variations in the content of pyroxene and feldspar is noticeable even in the hand sample. The microscopically determined mineral composition consists mainly of clinopyroxene, plagioclase, hornblende, epidote/clinozoisite, leukoxene and stilpnomelane. Alkali feldspar, apatite, titanite and zircon could be observed as accessories. The most common are subophitic texture (rocks with predominantly pyroxene) and intersertal texture (rocks with predominantly plagioclase, pyroxene then as gusset filling, [. . .])."

6.5.4 Dioritic dykes

Lithology numbers (58 | 52) in sheet (122 | 123)

"The term dioritic dykes (58) summarizes variants with a tendency towards intermediate chemistry. These metadiorites are especially significant as sills. [. . .]

In hand sample, the rocks appear massive, mostly fine-grained to dense. The rock color shows a medium grey. Occasionally, small feldspar-slats are identified on the fresh fractured rock surface. As a result, they are usually confused with greywacke beds. However, the leather-brown weathering color and occasional pyrite leads to a correct assignment in the field, which often had to be confirmed by thin sections.

The microscopically determined mineral composition consists mainly of plagioclase, hornblende, sericite, chlorite, pyroxene and epidote. Quartz and opaque minerals are subordinate in appearance. Apatite and zircon can be observed on accessories. The main components of the rock are hypidiomorphic, twinned, zonar plagioclase strips (about 1 mm long). They form a bulky irregular intersertal or intergranular structure. The interstices are filled with opaque minerals, sericite and chlorite; in addition, small hypidiomorphic hornblendes and isolated pyroxenes occur. Quartz is also part of the gusset fillings. It is not clear to decide whether it is primarily igneous quartz or metamorphic recrystallisation.

Due to the proximity to gabbros, the rocks are interpreted as product of differentiation."

6.6 Magnesite

Magnesite is not shown as a distinctive rock unit on the geological maps. Due to its major importance for this mapping project, the description of the magnesite occurring in the investigation area is taken from (Vavtar, 1976):

> "Magnesite occurs in a wide variety of color variations. There are all possible transitions from [...] red-colored to orange to yellow to dark brown and gray-colored magnesite. Three more distinctive types can be distinguished:
>
> 1. Yellow to grey-yellow magnesite with pyrite, goethite and lepidocrocite.
> 2. Red [...] magnesite with hematite and minor pyrite.
> 3. Gray to black magnesite with pyrite. [...]
>
> The magnesites differ not only in color but also in hardness. Bulky, relatively hard as well as porous, softer types coexist.
> Various factors are responsible for the different appearance of the magnesite:
>
> *Colouring pigment*: Sericite layers rich in hematite or the finest hematite-scales color the magnesite red. Locally, the hematite can be enriched to nodules parallel to the lamination. Pyrite-rich layers of sericite cause the magnesite to have a dark gray color. [...]
>
> *Weathering*: The magnesite is colored brown by weathering of the pyrite via lepidocrocite to goethite.
>
> *Recent magnesium mobilization*: Yellow magnesite can often be observed along joints, which partly extends into the bedding from such fine cracks and gives the magnesite a "cloudy" appearance. This is a more recent magnesium mobilization since the layered change in grain size that is otherwise often observed is absent and these magnesites are completely pigment-free even where they penetrate pigmented magnesite or extend parallel into layers.
>
> *Grain size change*: The rhythmic change in grain size can also cause grey-yellow layering of the magnesite. [...] In the rhythmic change in grain size, however, no polar or geopetal sructure in the form of vertical grain sorting can be determined."

Note: According to the current state of knowledge, the black coloring is due to a high proportion of organic carbon.

References

Angel, F., and Trojer, F., 1955, Zur Frage des Alters und der Genesis alpiner Spatmagnesite, *in* Radex-rundschau, Radenthein, Radex Austria A.G., v. 2, p. 374–392, https://opac.geologie.ac.at/ais312/dokumente/Radex-Rundschau_1955_374-392.pdf.

Azim Zadeh, A.M., Bakker, R.J., and Ebner, F., 2011, P-T conditions of fluid trapping at Hohentauern/Sunk sparry magnesite deposit (Eastern Alps, Austria), *in* Bakker, R.J., Baumgartner, M., and Doppler, G. eds., 21st biennial conference - european current research on fluid inclusions: ECROFI XXI: 9 - 11 august 2011 leoben austria: abstracts, Wien, Geologische Bundesanstalt, Berichte der geologischen bundesanstalt 87, p. 28–29, https://opac.geologie.ac.at/ais312/dokumente/BR0087_028_A.pdf.

Blatt, A., 2013, Geochronologische Datierung des Kellerjochgneises und der Porphyroide in der Nördlichen Grauwackenzone (Tirol, Österreich), *in* Mertmann, D., Degen, T., and Stöber, S. eds., Hallesches jahrbuch für geowissenschaften / beiheft, Institut für Geowissenschaften und Geographie der Martin-Luther-Universität Halle-Wittenberg, v. 29, doi:10.25673/90997.

Boggs, S., Jr., 2009, Petrology of Sedimentary Rocks: Cambridge University Press, 607 p., https://www.cambridge.org/9780521897167.

Deelman, J.C.C., 2020, Investigating magnesite from Austria: Research Report, https://hal.science/hal-02899916.

Haditsch, J.G., and Mostler, H., 1970, Die Kupfer-Nickel-Kobalt-Vererzung im Bereich Leogang (Inschlagalm, Schwarzleo, Nöckelberg), *in* Archiv für lagerstättenforschung in den ostalpen, Montanistische Hochschule Leoben, Institut für Mineralogie und Gesteinskunde, v. 11, p. 161–209, https://opac.geologie.ac.at/ais312/dokumente/ALO11_161_209.pdf.

Heinisch, H., 1981, Zum ordovizischen "Porphyorid" – Vulkanismus der Ost- und Südalpen, Stratigraphie, Petrographie, Geochemie, *in* Jahrbuch der geologischen bundesanstalt, Geologische Bundesanstalt (GBA), Wien, 1, v. 124, p. 1–109, https://opac.geologie.ac.at/ais312/dokumente/JB1241_001_A.pdf.

Heinisch, H., Pestal, G., and Reitner, J.M., 2015, Erläuterungen zu Blatt 122 Kitzbühl, *in* Geologische Karte der Republik Österreich 1:50.000: Erläuterung, Geologische Bundesanstalt (GBA), Wien, https://opac.geologie.ac.at/ais312/dokumente/122_Kitzbuehel.pdf.

Heinisch, H., Pestal, G., Reitner, J., and Stingl, V., 2003, Blatt 122 Kitzbühl, *in* Geologische karte der republik Österreich 1:50.000, Geologische Bundesanstalt (GBA), Wien, https://opac.geologie.ac.at/ais312/dokumente/GK0122_000_A.pdf.

Heinisch, H., Pestal, G., Stingl, V., and Hellerschmidt-Alber, J., 1995, Blatt 123 Zell am See, *in* Geologische karte der republik Österreich 1:50.000, Geologische Bundesanstalt (GBA), Wien, https://opac.geologie.ac.at/ais312/dokumente/GK0123_000_A.pdf.

Henjes-Kunst, F., Prochaska, W., Niedermayr, A., Sullivan, N., and Baxter, E., 2014, Sm-Nd dating of hydrothermal carbonate formation: An example from the Breitenau magnesite deposit

(Styria, Austria): Chemical Geology, v. 387, p. 184–201, doi:10.1016/j.chemgeo.2014.07.025.

Hubmann, B., Ebner, F., Ferretti, A., Kido, E., Krainer, K., Neubauer, F., Schönlaub, H.-P., and Suttner, T.J., 2014, The Paleozoic Era(them), *in* Piller, W. ed., The lithostratigraphic units of the austrian stratigraphic chart 2004 (sedimentary successions), Geologische Bundesanstalt (GBA), Wien, Abhandlungen der geologischen bundesanstalt, v. 66, https://opac.geologie.ac.at/ais312/dokumente/AB0066_001_A.pdf.

Huet, B., Iglseder, C., and Schuster, R., 2022, A lithostratigraphic model for the Western Greywacke Zone and the Innsbruck Quarzphyllite Zone (Eastern Alps, Tirol, Salzburg, Austria) (G. Rantitsch & J. G. Raith, Eds.):, https://opac.geologie.ac.at/ais312/dokumente/Pangeo_Austria_2022_078.pdf.

Huet, B., Iglseder, C., and Schuster, R., 2019, Eine neue tektonische und lithostratigrafische Gliederung im Ostalpin auf der Geologischen Karte der Republik Österreich 1:50.000, Blatt 121 Neukirchen am Großvenediger:, https://opac.geologie.ac.at/ais312/dokumente/ATA-2019_221.pdf.

Le Maitre, R.W. et al., 2002, Igneous Rocks: A Classification and Glossary of Terms: Recommendations of the International Union of Geological Sciences Subcommission on the Systematics of Igneous Rocks (R. W. Le Maitre, Ed.): Cambridge, Cambridge University Press, doi:10.1017/CBO9780511535581.

Mavridis, A., 1969, Geologie der Umgebung des Spielberghornes (Nördliche Grauwackenzone, Tirol - Salzburg), *in* Kurzfassungen von in innsbruck fertiggestellten dissertationen (1965-1977); teil 1, Geologisch-Paläontologische Mitteilungen Innsbruck, p. 28–30, https://opac.geologie.ac.at/ais312/dokumente/GPM_06_10_028-030.pdf.

Mavridis, A., and Mostler, H., 1971, Zur Geologie der Umgebung des Spielberghorns mit einem Beitrag über die Magnesitvererzung (Nördliche Grauwackenzone, Tirol-Salzburg), *in* Mostler, H. ed., Beiträge zur mikrofazies und stratigraphie von tirol und vorarlberg 1971, Innsbruck, Universitätsverlag Wagner, p. 523–546.

Mayer-Jauck, H., and Schatz, M., 2023, Österreichisches Montan-Handbuch: Wien, Bundesministerium für Finanzen, v. 96, https://www.bmf.gv.at/dam/jcr:4abaabea-0c4b-4600-9415-939756f0a79a/MHB 2022_barrierefrei_V1.pdf.

McCann, T., and Manchego, M.V., 2015, Geologie im Gelände: Springer Berlin Heidelberg, doi:10.1007/978-3-8274-2383-2.

Morteani, G., 1989, Mg-metasomatic type sparry magnesites of Entachen Alm, Hochfilzen/Bürglkopf and Spiessnägel (Austria) (P. Möller, Ed.): Berlin, Borntraeger, Monograph series on mineral deposits 28, p. 105–113.

Morteani, G., Moeller, P., and Schley, F., 1982, The rare earth element contents and the origin of the sparry magnesite mineralizations of Tux-Lanersbach, Entachen Alm, Spiessnaegel, and Hochfilzen, Austria, and the lacustrine magnesite deposits of Aiani-Kozani, Greece, and Bela Stena, Yugoslavia: Economic Geology, v. 77, p. 617–631, doi:10.2113/gsecongeo.77.3.617.

Morteani, G., and Neugebauer, H., 1990, Chemical and tectonic controls on the formation of sparry magnesite deposits - the deposits of the northern Greywacke Zone (Austria): Geologische Rundschau, v. 79, p. 337–344, doi:10.1007/bf01830630.

Mostler, H., 1973, Alter und Genese ostalpiner Spatmagnesite unter besonderer Berücksichtigung der Magnesitlagerstätten im Westabschnitt der Nördlichen Grauwackenzone (Tirol, Salzburg), *in* Festschrift werner heißel zum 65. geburtstag, Universität Innsbruck, p. 237–266, https://opac.geologie.ac.at/ais312/dokumente/Mostler_1973_Spatmagnesite_Grauwackenzone.pdf.

Mostler, H., 1970, Ein Beitrag zu den Magnesitvorkommen im Westabschnitt der nördlichen Grauwackenzone (Tirol und Salzburg), *in* Archiv für lagerstättenforschung in den ostalpen, Montanistische Hochschule Leoben, Institut für Mineralogie und Gesteinskunde, v. 11, p. 113–125, https://opac.geologie.ac.at/ais312/dokumente/ALO11_113_125.pdf.

Nichols, G., 2009, Sedimentology and stratigraphy: Chichester [u.a.], Wiley-Blackwell, 419 p.

North American Commission on Stratigraphic Nomenclature, 2005, North American Stratigraphic Code: AAPG Bulletin, v. 89, p. 1547–1591, doi:10.1306/07050504129.

Panwitz, C., 2006, Provenienzanalyse an paläozoischen Metasedimenten der Ostalpen mit Schwerpunkt in der Nördlichen Grauwackenzone [PhD thesis]: Martin-Luther-Universität Halle-Wittenberg, doi:10.23689/FIDGEO-198.

Pohl, W.L., 2020, Economic Geology: Principles and Practice. Metals, Minerals, Coal and Hydrocarbons - Introduction to Formation and Sustainable Exploitation of Mineral Deposits: Stuttgart, Germany, Schweizerbart Science Publishers, 755 p., http://www.schweizerbart.de//publications/detail/isbn/9783510654413/Pohl/_Economic/_Geology/_2/_Aufl/_geb.

Pohl, W., 1990, Genesis of magnesite deposits – models and trends: Geologische Rundschau, v. 79, p. 291–299, doi:10.1007/bf01830626.

Prochaska, W., 2016, Genetic concepts on the formation of the Austrian magnesite and siderite mineralizations in the Eastern Alps of Austria: Geologia Croatica, v. 69, p. 31–38, doi:10.4154/gc.2016.03.

Prochaska, W., 2001, Magnesite mineralization of the Eastern Alps and the Carpathians, *in* Piestrzyński, A. ed., Mineral deposits at the beginning of the 21st century, London, CRC Press, p. 1017–1019, doi:10.1201/9781003077503-260.

Rantitsch, G., and Judik, K., 2009, Alpine metamorphism in the central segment of the Western Greywacke Zone (Eastern Alps): Geologica Carpathica, v. 60, p. 319–329, doi:10.2478/v10096-009-0023-2.

Riedler, E., 2010, Geologische Charakterisierung und 3D-Modellierung des Magnesitvorkommens Bürglkopf (Hochfilzen/Tirol; westliche Grauwackenzone) [Master's thesis]: Montanuniversität Leoben, https://puretest.unileoben.ac.at/files/1909816/AC08216179n01vt.pdf.

Schaen, A.J. et al., 2020, Interpreting and reporting 40Ar/39Ar geochronologic data: GSA Bulletin, doi:10.1130/B35560.1.

Schlaegel-Blaut, P., 1990, Der basische Magmatismus der Nördlichen Grauwackenzone, Oberostalpines Paläozoikum: Geologische Bundesanstalt (GBA), Wien, Abhandlungen der geologischen bundesanstalt, v. 43, https://opac.geologie.ac.at/ais312/dokumente/AB0043_001_A.pdf.

Schmid, S.M., Fügenschuh, B., Kissling, E., and Schuster, R., 2004, Tectonic map and overall architecture of the Alpine orogen: Eclogae Geologicae Helvetiae, v. 97, p. 93–117, doi:10.1007/s00015-004-1113-x.

Schulz, O., and Vavtar, F., 1989, Genetic fabric interpretation of the magnesite deposit of Weißenstein (Hochfilzen, Tyrol) (P. Möller, Ed.): Berlin, Borntraeger, Monograph series on mineral deposits 28, p. 115–134.

Schuster, R., 2015, Grauwackenzone und Veitsch-Silbersberg-Deckensystem:, p. 38–43, https://opac.geologie.ac.at/ais312/dokumente/ATA2015_Auflage_2_038.pdf.

Schuster, R., Daurer, A., Krenmayr, H.G., Linner, M., Mandl, G.W., Pestal, G., and Reitner, J.M., 2015, Rocky Austria: Geologie von Österreich-kurz und bunt: Geologische Bundesanstalt (GBA), Wien.

Schuster, R., Koller, F., Hoeck, V., Hoinkes, G., and Bousquet, R., 2004, Explanatory notes to the map: Metamorphic structure of the Alps – Metamorphic evolution of the Eastern Alps: Mitteilungen der Österreichischen Mineralogischen Gesellschaft, v. 149, p. 175–199, https://opac.geologie.ac.at/ais312/dokumente/Mitt_OEMinGes_149_175-199.pdf.

Schuster, R., Kurz, W., Krenn, K., and Fritz, H., 2013, Introduction to the Geology of the Eastern Alps, *in* Schuster, R. ed., 11th workshop on alpine geological studies & 7th european symposium on fossil algae: Abstracts & field guides, Wien, Geologische Bundesanstalt (GBA), Berichte der geologischen bundesanstalt 99, p. 121–133, https://opac.geologie.ac.at/ais312/dokumente/BR0099_121_A.pdf.

Schuster, R., and Stüwe, K., 2022, Geological and Tectonic Setting of Austria, *in* Embleton-Hamann, C. ed., Landscapes and landformsof austria, Springer International Publishing, World geomorphological landscapes, p. 3–26, doi:10.1007/978-3-030-92815-5_1.

Siegl, W., 1964, Die Magnesite der Werfener Schichten im Raume Leogang bis Hochfilzen sowie Ellmau in Tirol, *in* Radex-rundschau, Radenthein, Radex Austria A.G., v. 3, p. 178–191, https://opac.geologie.ac.at/ais312/dokumente/Radex-Rundschau_1964_178-191.pdf.

Siegl, W., 1953, Magnesit in den Werfener Schichten bei Leogang, *in* Österreichische akademie der wissenschaften mathematisch-naturwissenschaftliche klasse anzeiger, Wien, Springer, v. 90, p. 178–180.

Spötl, C., and Burns, S.J., 1994, Magnesite diagenesis in redbeds: a case study from the Permian of the Northern Calcareous Alps (Tyrol, Austria): Sedimentology, v. 41, p. 543–565, doi:10.1111/j.1365-3091.1994.tb02010.x.

Tollmann, A., 1977, Geologie von Österreich: Band I: Die Zentralalpen: Deuticke, Wien.

Vavtar, F., 1976, Gefügeanalytische Untersuchungen der Magnesitlagerstätte Bürglkopf – Weißenstein bei Hochfilzen, Tirol, *in* Verhandlungen der geologischen bundesanstalt, Wien, Geologische Bundesanstalt (GBA), Verhandlungen der geologischen bundesanstalt 2, p. 147–182, https://opac.geologie.ac.at/ais312/dokumente/VH1976_147_A.pdf.

Vinx, R., 2015, Gesteinsbestimmung im Gelände: Springer Spektrum, doi:10.1007/978-3-642-55418-6.

INTERNATIONAL CHRONOSTRATIGRAPHIC CHART

IUGS

www.stratigraphy.org | **International Commission on Stratigraphy** | **v 2023/09**

Eonothem / Eon	Erathem / Era	System / Period	Series / Epoch		Stage / Age	numerical age (Ma)
						present
Phanerozoic	Cenozoic	Quaternary	Holocene	U/L	Meghalayan	0.0042
				M	Northgrippian	0.0082
				L/E	Greenlandian	0.0117
			Pleistocene	U/L	*Upper*	0.129
				M	Chibanian	0.774
				L/E	Calabrian	1.80
					Gelasian	2.58
		Neogene	Pliocene	U/L	Piacenzian	3.600
				L/E	Zanclean	5.333
			Miocene	U/L	Messinian	7.246
					Tortonian	11.63
				M	Serravallian	13.82
					Langhian	15.98
				L/E	Burdigalian	20.44
					Aquitanian	23.03
		Paleogene	Oligocene		Chattian	27.82
					Rupelian	33.9
			Eocene		Priabonian	37.71
					Bartonian	41.2
					Lutetian	47.8
					Ypresian	56.0
			Paleocene		Thanetian	59.2
					Selandian	61.6
					Danian	66.0
	Mesozoic	Cretaceous	Upper		Maastrichtian	72.1 ±0.2
					Campanian	83.6 ±0.2
					Santonian	86.3 ±0.5
					Coniacian	89.8 ±0.3
					Turonian	93.9
					Cenomanian	100.5
			Lower		Albian	~ 113.0
					Aptian	~ 121.4
					Barremian	125.77
					Hauterivian	~ 132.6
					Valanginian	~ 139.8
					Berriasian	~ 145.0

Eonothem / Eon	Erathem / Era	System / Period	Series / Epoch	Stage / Age	numerical age (Ma)
					~ 145.0
Phanerozoic	Mesozoic	Jurassic	Upper	Tithonian	149.2 ±0.7
				Kimmeridgian	154.8 ±0.8
				Oxfordian	161.5 ±1.0
			Middle	Callovian	165.3 ±1.1
				Bathonian	168.2 ±1.2
				Bajocian	170.9 ±0.8
				Aalenian	174.7 ±0.8
			Lower	Toarcian	184.2 ±0.3
				Pliensbachian	192.9 ±0.3
				Sinemurian	199.5 ±0.3
				Hettangian	201.4 ±0.2
		Triassic	Upper	Rhaetian	~ 208.5
				Norian	~ 227
				Carnian	~ 237
			Middle	Ladinian	~ 242
				Anisian	247.2
			Lower	Olenekian	251.2
				Induan	251.902 ±0.024
	Paleozoic	Permian	Lopingian	Changhsingian	254.14 ±0.07
				Wuchiapingian	259.51 ±0.21
			Guadalupian	Capitanian	264.28 ±0.16
				Wordian	266.9 ±0.4
				Roadian	273.01 ±0.14
			Cisuralian	Kungurian	283.5 ±0.6
				Artinskian	290.1 ±0.26
				Sakmarian	293.52 ±0.17
				Asselian	298.9 ±0.15
		Carboniferous	Pennsylvanian Upper	Gzhelian	303.7 ±0.1
				Kasimovian	307.0 ±0.1
			Pennsylvanian Middle	Moscovian	315.2 ±0.2
			Pennsylvanian Lower	Bashkirian	323.2 ±0.4
			Mississippian Upper	Serpukhovian	330.9 ±0.2
			Mississippian Middle	Visean	346.7 ±0.4
			Mississippian Lower	Tournaisian	358.9 ±0.4

Eonothem / Eon	Erathem / Era	System / Period	Series / Epoch	Stage / Age	numerical age (Ma)
					358.9 ±0.4
Phanerozoic	Paleozoic	Devonian	Upper	Famennian	372.2 ±1.6
				Frasnian	382.7 ±1.6
			Middle	Givetian	387.7 ±0.8
				Eifelian	393.3 ±1.2
			Lower	Emsian	407.6 ±2.6
				Pragian	410.8 ±2.8
				Lochkovian	419.2 ±3.2
		Silurian	Pridoli		423.0 ±2.3
			Ludlow	Ludfordian	425.6 ±0.9
				Gorstian	427.4 ±0.5
			Wenlock	Homerian	430.5 ±0.7
				Sheinwoodian	433.4 ±0.8
			Llandovery	Telychian	438.5 ±1.1
				Aeronian	440.8 ±1.2
				Rhuddanian	443.8 ±1.5
		Ordovician	Upper	Hirnantian	445.2 ±1.4
				Katian	453.0 ±0.7
				Sandbian	458.4 ±0.9
			Middle	Darriwilian	467.3 ±1.1
				Dapingian	470.0 ±1.4
			Lower	Floian	477.7 ±1.4
				Tremadocian	485.4 ±1.9
		Cambrian	Furongian	*Stage 10*	~ 489.5
				Jiangshanian	~ 494
				Paibian	~ 497
			Miaolingian	Guzhangian	~ 500.5
				Drumian	~ 504.5
				Wuliuan	~ 509
			Series 2	*Stage 4*	~ 514
				Stage 3	~ 521
			Terreneuvian	*Stage 2*	~ 529
				Fortunian	538.8 ±0.2

Eonothem / Eon	Erathem / Era	System / Period	numerical age (Ma)
			538.8 ±0.2
Precambrian – Proterozoic	Neoproterozoic	Ediacaran	~ 635
		Cryogenian	~ 720
		Tonian	1000
	Mesoproterozoic	Stenian	1200
		Ectasian	1400
		Calymmian	1600
	Paleoproterozoic	Statherian	1800
		Orosirian	2050
		Rhyacian	2300
		Siderian	2500
Precambrian – Archean	Neoarchean		2800
	Mesoarchean		3200
	Paleoarchean		3600
	Eoarchean		4031 ± 3
Hadean			4567

Units of all ranks are in the process of being defined by Global Boundary Stratotype Section and Points (GSSP) for their lower boundaries, including those of the Archean and Proterozoic, long defined by Global Standard Stratigraphic Ages (GSSA). Italic fonts indicate informal units and placeholders for unnamed units. Versioned charts and detailed information on ratified GSSPs are available at the website http://www.stratigraphy.org. The URL to this chart is found below.

Numerical ages are subject to revision and do not define units in the Phanerozoic and the Ediacaran; only GSSPs do. For boundaries in the Phanerozoic without ratified GSSPs or without constrained numerical ages, an approximate numerical age (~) is provided.

Ratified Subseries/Subepochs are abbreviated as U/L (Upper/Late), M (Middle) and L/E (Lower/Early). Numerical ages for all systems except Quaternary, upper Paleogene, Cretaceous, Jurassic, Triassic, Permian, Cambrian and Precambrian are taken from 'A Geologic Time Scale 2012' by Gradstein et al. (2012), those for the Quaternary, upper Paleogene, Cretaceous, Jurassic, Triassic, Permian, Cambrian and Precambrian were provided by the relevant ICS subcommissions.

Colouring follows the Commission for the Geological Map of the World (www.ccgm.org)

CCGM CGMW

Chart drafted by K.M. Cohen, D.A.T. Harper, P.L. Gibbard, N. Car

To cite: Cohen, K.M., Finney, S.C., Gibbard, P.L. & Fan, J.-X. (2013; updated) The ICS International Chronostratigraphic Chart. Episodes 36: 199-204.

URL: http://www.stratigraphy.org/ICSchart/ChronostratChart2023-09.pdf